A WIRELESS VLF DIGITAL COMMUNICATION UPLINK FOR COAL MINES USING SS MODULATION

by

S. V. RAVI KUMAR

DEPARTMENT OF ELECTRICAL ENGINEERING
INDIAN INSTITUTE OF TECHNOLOGY, KANPUR

AUGUST 1984

18/8/84

CERTIFICATE

It is to certify that the thesis entitled, 'A WIRELESS VLF DIGITAL COMMUNICATION UPLINK FOR COAL MINES USING SS MODULATION', submitted by Mr. S.V. Ravi Kumar, Roll No.8210431, for the partial fulfilment of the requirements for the award of M.Tech. degree, has been carried out under my supervision. According to my knowledge, it has not been submitted elsewhere for an award of a degree.

R. Raghuram
18/8/84

(R. Raghuram)
Assistant Professor
Department of Electrical Engg.
I.I.T. Kanpur.

ACKNOWLEDGEMENTS

I express my deep sense of gratitude to Dr. R. Raghuram for his invaluable guidance and appreciation throughout the course of my thesis work.

I am thankful to Dr. K.R. Sarma for suggesting me this project. I am thankful to Dr. P.R.K. Rao and Dr. K.R.Srivathsan for their timely suggestions. I am very thankful to my friends S.V. Rao and B.V. Rao who helped me a lot throughout my thesis work. I am thankful to V.V.S. Murthy, B.V.N. Kumar ~~and~~ S.S.R. Murthy, Gaya Prasad, and Krishna Swamy who helped me in the final preparation of my thesis.

Finally, I thank Mr. C.M. Abraham for his efficient typing work.

S.V. Ravi Kumar

ABSTRACT

Communication systems in mines involving cables are prone to get damaged especially at the time of disaster. Hence wireless Very Low Frequency (VLF) links have found application. The low power transmitter has to operate from the miners caplamp battery which has a voltage of 3.5 - 4V. Basically a modulation scheme which suits the requirement of low power transmission and large amount of interference rejection is to be employed. A comparison of the various systems has been made. A coherent scheme using spread spectrum is proposed here. Using spread spectrum each substation in the mine can be operated simultaneously on noninterference basis by assigning different codes to them. Based on the noise models derived, a biphase modulated direct sequence speread spectrum communication system has been constructed. The wireless communication link can be used for routine as well as for emergency communication.

TABLE OF CONTENTS

CHAPTER 1

INTRODUCTION

1.1 BASIC NEEDS AND SPECIFICATIONS OF MINES COMMUNICATION SYSTEM

Communication systems in mines involving cables are prone to get damaged especially at the time of disaster. Further the practicability of installing coaxial cables in the working area of the mine seems questionable. However, the normal radio frequencies used for wireless transmission cannot be used in mines because of the limited depth of penetration. Very low frequency (VLF - 3 to 30 kHz) and extra low frequency (ELF - 30 Hz to 3 kHz) have therefore been used. The background noise and interference from mine equipment become troublesome at VLF particularly for wideband systems such as voice transmissions. This is especially true for uplink (mine to surface communication) as the transmitter has to operate from the miners caplamp battery which has a voltage of 3.5 - 4V. The communication link can't be voice because of the power drainage and large bandwidth problems. The objective of this work is to design and construct a wireless digital data communication uplink i.e. from subsurface to surface through the earth using inductively coupled electromagnetic fields.

At the surface the receiver has to combat with two sources of noise the manmade noise which is dominant and the atmospheric noise. To cover depths of 300 m the signal level available at the surface is almost comparable with noise level. So a receiver using correlation techniques will be useful to improve signal detectability [1]. The operating range of an underground radio communication system depends upon many factors including : the signal propagation mechanism and medium, antenna system gain or coupling efficiency, transmitter output power, characteristics of electrical noise generated in the mine electrical system, susceptability of the receiver to desensitization by electrical noise and other interfering/ jamming signals and the system modulation demodulation processes.

Available signal to noise ratios apart from frequency, pathlength, transmitting power also depends on conductivity of earth. Earth is assumed to be a homogeneous, isotropic medium with an average conductivity of 0.01 mhos/m for most of the applications done here.

The crucial requirements for a transmitter for the uplink are as follows :

1. It should be small, compact and light weight
2. It should be easy to use since the miner may be illiterate

3. It should have a low power drainage, since it is to be run from the miners headlamp battery and it must not substantially effect battery life.

The class B power amplifier at the transmitter can supply a maximum current of 1 Ampere through the loop. As the transmitting loop is mounted on a square pillar of 25 m side, the transmitting antenna magnetic moment can't be increased more than 625 Ampere turns.

1.2 DESCRIPTION OF THE THROUGH THE EARTH UPLINK COMMUNICATION SYSTEM

A schematic of the through the earth communication system is shown in Fig. 1.1. The antennas employed here are coaxial loops. Three components of the H field should be measured but of these the vertical component is dominant near the axis. This is because the direction of transmission will usually be vertical and also because the atmospheric noise and other noise components will be less for the vertical component than for either horizontal component. The position of the underground transmitter was determined by measuring the horizontal signal field at different locations and by finding null in the field, the underground transmitter was found by triangulation.

The quantity that should be measured is magnetic field strength H. The reason for using H-field measurements is that

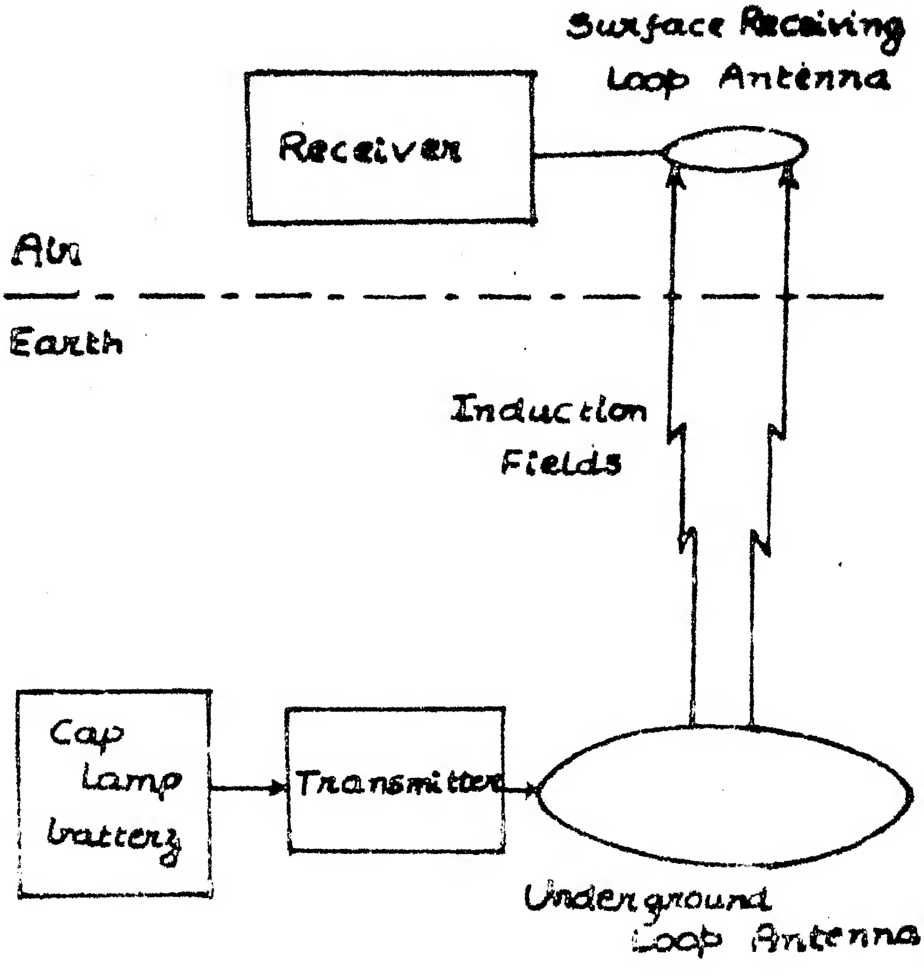

[illegible] Schematic of the Uplink System

the transfer of energy is via magnetic field for frequencies $<$ 100 kHz as the following argument shows. It must be remembered that the transfer of power is through induction fields. At any air-ground interference where η_1 is the intrinsic impedance of the air and η_2 is the intrinsic impedance of ground, a standing wave pattern is setup.

$$\text{VSWR} = \frac{1 + |\Gamma|}{1 - |\Gamma|} \text{ where}$$

the reflection coefficient $|\Gamma| = \dfrac{\eta_2 - \eta_1}{\eta_2 + \eta_1}$

For $\eta_2 < \eta_1$, the incident and reflected components of the magnetic field add and hence the resultant magnetic field is enhanced at the interface. Thus the predominant source of energy in the ground is in the magnetic field [2].

An antenna immersed in an H field will convert the energy from the magnetic field into current in load and the resulting voltage or power is what is actually measured. If an N turn loop antenna of cross sectional area A is immersed in a magnetic field H at angular frequency ω in an isotropic medium of permeability μ where the normal to the plane of the loop is at an angle ψ from the magnetic field, the magnitude of induced open circuit voltage is

$$V_{oc} = \omega\mu HAN \cos\psi$$

The amplitude probability distribution (APD) curves given as the % of time the received noise envelope exceeds the various level for that particular receiver bandwidth are very useful for digital systems operating in noise environment [3]. The APD measurements can be used to convert average field strength measurements to available power density (RMS field).

The antenna equivalent circuit has been shown in Fig. 1.2.
R_1 = Antenna Resistance
At the lower frequencies < 50-100 kHz the copper losses are much greater than the loss due to radiation resistance. So the antenna resistance can be approximated by the copper losses.

The resistance of the transmitting loop (No. 18 wire) of radius 15 m is calculated to be 3.45 ohms. The inductance is calculated to be 3.59×10^{-4} Henrys.

The input impedance may be resistive and equal to R_1 by correct selection of an external capacitance C_1 placed in series with the antenna.

In Fig. 1.2,

$$V_2 = E \cos(\omega t - \frac{r}{\delta} - \pi)$$

where ω = signalling frequency in radians/sec.

r = distance between antennas

= skin depth of earth at operating frequency.

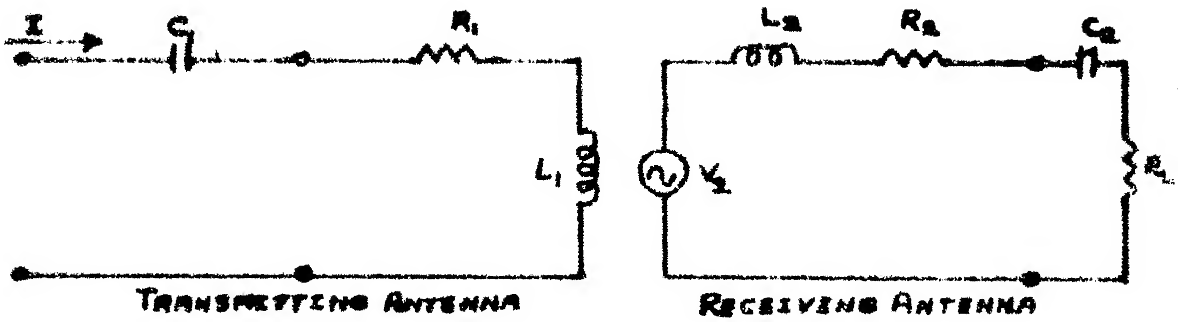

FIG 1.2 ANTENNA EQUIVALENT CIRCUIT

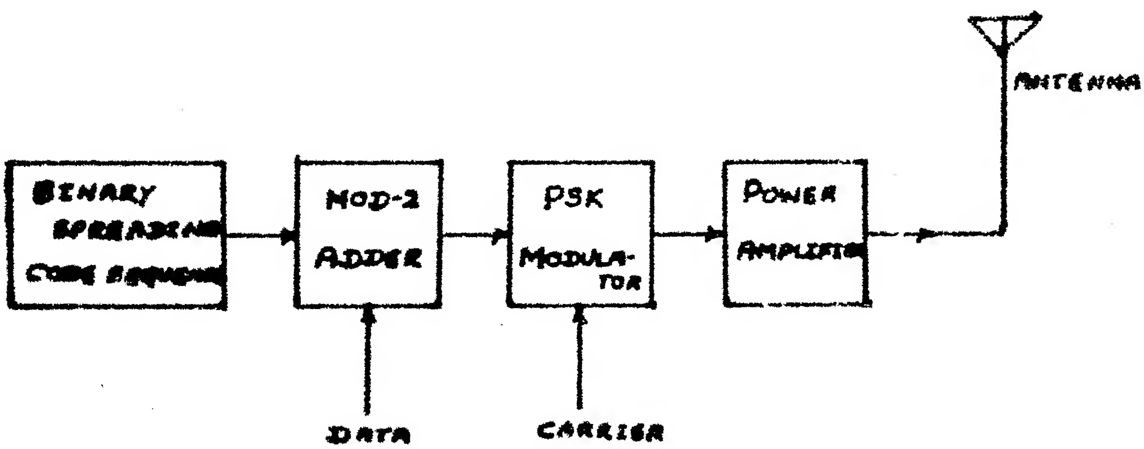

FIG 1.3 BIPHASE PM MODULATOR/ TRANSMITTER

1.3 BRIEF DESCRIPTION OF EXISTING COMMUNICATION SYSTEMS

1.3.1 Voice Uplink Via Phone Line with Paging Capability [4]

This is an optional feature which permits coupling the surface and subsurface stations to existing phone lines in the mine when available. A handset and paging switch and paging relay is provided at both the terminals. Depressing the page switch on a conventional pager which is connected by phone line to the subsurface station applies power to the circuitry and permits the pagers voice signals to be transmitted through the earth from the subsurface unit.

1.3.2 Voice Uplink Using Narrow Band FM through-the-earth Signals [5]

The subsurface station includes handset microphone and preamplifier whose output is connected to the phone line (when used) and to a voltage controlled oscillator to generate the NBFM signals using a carrier frequency of 7 kHz. The output of the VCO is connected to the power amplifier through a switch mode selector only when the press to talk on the handset switch is depressed. On the surface it is necessary to deploy and couple to the receiver one or more antennas. Antenna outputs can be connected separately or together and their outputs are summed in the antenna coupler. Switches are provided on the front panel to select the desired antenna configuration.

1.3.3 Condition Monitoring Uplink [6]

The six bit codeword corresponding to one of three condition levels NORMAL, CAUTION and ALARM is transmitted 16 times in 19.2 seconds every 10.2 minutes or whenever a condition threshold level changes. The condition code is used to frequency shift the data carrier frequency. At the receiver the signal is filtered, decoded and the binary key stream compared with similar codes stored in the PCM decoder register. Each time the incoming key stream matches the register code a pulse is generated when four such pulses out of a possible six are received during a transmission interval the status light corresponding to that received code is illuminated. Three lights are used for the three conditions. Under ALARM conditions the red light is turned on and an audible tone is heard in the loud speaker.

1.3.4 Coded Beacon Uplink [6]

This is an emergency feature of the system which permits the operator to transmit coded responses by manually depressing a push button at the subsurface station corresponding to the response desired. Six responses are available. These are. YES, NO, DON'T KNOW, REPEAT, WAIT and MORSE CODE FOLLOWS. A separate CODE KEY button is provided for sending the Morse code when desired. This button activates the carrier only when depressed.

When one of the coded response buttons is depressed a 6 bit binary code is generated and repeated for the period of the time the button is depressed. This code stream is used to frequency shift a key a carrier for subsequent transmission. Upon reception the FSK signal is detected and decoded and visually indicated with a rear projection display which lights up the word corresponding to the button depressed.

Each subsurface station is assigned a specific carrier frequency for data transmission to permit station identification and simultaneous operation on a noninterference basis. The assigned frequencies are selected to fall between the 50 Hz harmonic noise frequencies.

1.3.5 On-Off Signalling

This scheme has been already tested at the mine site here. Interrupted continuous wave transmissions in the range of 500 Hz to 15 kHz have been used. Typical transmissions have been of the type .1 sec on and 0.9 sec off.

1.4 DESCRIPTION OF SPREAD SPECTRUM [7]

The essense of spread spectrum communications - the art of expanding the bandwidth of a signal, transmitting that expanded signal, and recovering the desired signal by remapping the received spread spectrum into the original information bandwidth.

The basis of spread spectrum technology is expressed by C.E. Shannon in the form of channel capacity :

$$C = W \log_2(1 + \frac{S}{N})$$

where C = capacity in bits/see

N = noise power

W = bandwidth in Hertz

S = signal power

Letting C be the desired system information rate,

$$\frac{C}{W} = 1.44 \text{ Log}_e \ (1 + \frac{S}{N})$$

For $\frac{S}{N}$ small, say $\leq$ .1

$$\frac{C}{W} = 1.44 \frac{S}{N} \text{ (by logarithmic expansion)}$$

or

$$W = \frac{NC}{1.44 S}$$

We see that for any given noise to signal ratio we can have a low information error rate by increasing the bandwidth used to transfer the information.

The schematic of the Direct code modulation spread spectrum has been shown in Fig. 1.3.

The information is being added to the spectrum spreading code before it is used for spreading modulation. The information to be sent must be in some digital form in this

process because addition to a code sequence involves modulo-2 addition to a binary code as shown in Fig. 1.3. The need in spread spectrum (SS) systems is often to output a constant-power RF envelope. So some form of angle modulation PSK or FSK is usually employed. The SS signal is despread at the receiver by correlating the received signals with a local reference signal identical to that code used for signal spreading at the transmitter and the wanted spread signal collapses to its original bandwidth. Signals which are not correlated with the spreading code are spread by the local reference signal to its bandwidth, or more, and a narrowband filter then suppresses the effects of all but the wanted signal.

The receiver must acquire and track the PN code before carrier tracking and data demodulation takes place. The passive correlator acquires the PN code to within a chip time (Initial Synchronisation) and the active correlator or code tracking loop refines the delay estimate. There are two code tracking configurations, the delay locked loop (DLL) and the tau-dither loop. The DLL which is the optimum tracker achieves a linear error detector characteristic by subtracting an advanced (by γ seconds) correlation from a delayed correlation.

In spread spectrum processors the process gain available may be

$$\text{Process Gain} = G_p = \left[\frac{(S/I)_{out}}{(S/I)_{in}}\right]$$

$$= \frac{S/I \ B_m}{S/I \ B_c}$$

$$= \frac{B_c}{B_m} = \frac{R_c}{R_i}$$

where

B_c = SS bandwidth

B_m = Information bandwidth

R_c = Code rate

R_i = Information rate

There are many reasons for spreading the spectrum and a multiplicity of benefits can accrue simultaneously. Some of these are Antiinteference, Low probability of intercept, Multi-user random access communications with selective addressing capability, high resolution ranging.

1.5 CHOICE OF SS MODULATION IN MINES COMMUNICATIONS

Unlike the VLF radio wave propagation wherein the bandwidth is limited to about 50 Hz, Bandwidth is not a serious constraint for VLF through the earth as values of Q for the antenna are of the order of 1. For 18 Gauge Copper wire at a centre frequency of 2.5 kHz the antenna bandwidth is approximately 1530 Hz.

At the surface the predominant source of noise is power line harmonic interference as can be seen from Fig. 1.4. Considerable mine depths (= 1000 ft) cannot be covered as this noise is almost comparable to the signal level available at the surface. Spread spectrum modulating processes have the ability to increase the recovered output signal to noise ratio by providing process gain in the communication channel.

Assuming the atmospheric noise as white Gaussian over the band of interest, SS will neither improve nor deteriorate the performance as far as atmospheric noise is concerned. The existing [8] FSK schemes (coherent or noncoherent) have problems due to power line harmonic interference. The frequency instability of power line frequency makes selection of carrier frequencies difficult. A theoretical analysis for how the SS improves against power line harmonic interference has been done. On the basis of this, SS is feasible under such interference.

Using SS each substation in the mine can be operated, simultaneously on noninterference basis by assigning different codes to them.

1.6 The various chapters are organised in the following manner.

Chapter 2 describes the theoretical analysis of the spread spectrum system.

10

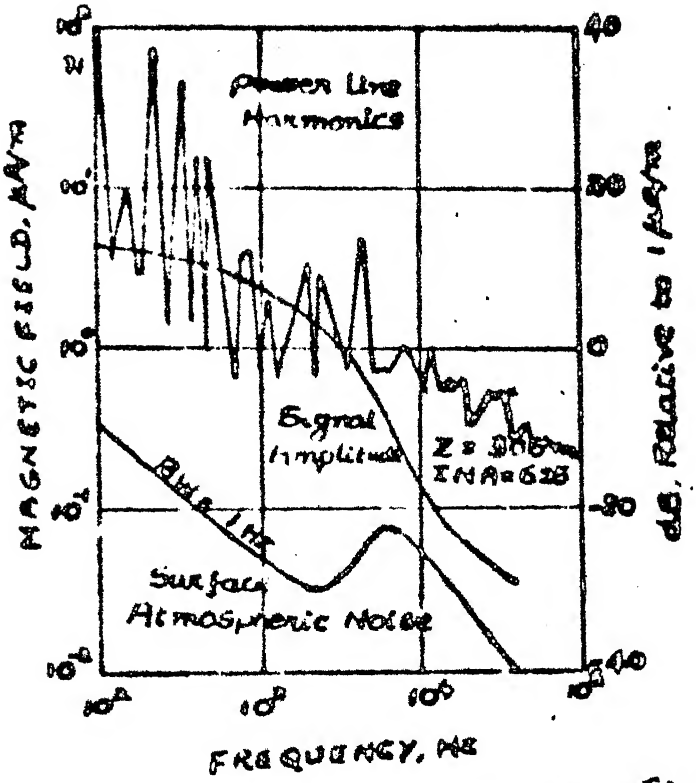

Fig. 4. Surface Noise and Signal Strength.

Chapter 3 describes the VLF transmitter for synchronous and asynchronous transmissions using SS modulation.

Chapter 4 describes the design and construction of the VLF receiver.

Chapter 5 gives the suggestions for future work and conclusions.

CHAPTER 2

DESIGN CONSIDIERATIONS

2.1 THE MINE NOISE ENVIRONMENT

The performance of any communication system is ultimately limited by noise which perturbs the received signal and causes errors in data. This noise is an additive disturbance either natural or manmade whose effects can be reduced by increasing the signal power by proper signal design and by noise suppression circuitary.

Low frequency electromagnetic systems used for through the earth communications in mines must contend with three basic types of noise, thermal, atmospheric and manmade. Thermal noise generated by resistance in the antenna and front end circuits determines the receiver's ultimate sensitivity. Atmospheric noise is a natural occurrence caused by lightning strokes. Manmade noise is probably the worst offender in mines. It is usually caused by the mine equipment itself and can severely limit the performance of receivers operating near the working face.

The three types of noise thermal, atmospheric and manmade all have different characteristics. The average power of thermal noise is usually fairly constant throughout

the lower frequency bands, where as the atmospheric and manmade noise may vary considerably with frequency. The probability density distribution of thermal noise is typically Gaussian.Atmospheric noise on the otherhand contains intermittent impulses superimposed on a Gaussian noise background. The characteristics of manmade mine noise vary considerably but the observed spectrum usually contains several discrete frequency components which vary in amplitude. This continuous wave interference generally occurs at 50 Hz and various harmonics of 50 Hz extending to several KHz.

Thermal noise can limit the sensitivity of surface receiver unless a proper choice of receiver antenna and front-end configuration has been made, so that acceptable signal-to-noise ratios are achieved.

The performance of a wideband system with receiver on the surface will be greatly limited by atmospheric noise. A considerable reduction in the effects of atmospheric noise can be achieved by clipping noise peaks in wideband circuits preceeding the bandlimiting portions of the receiver. The clipping process however is ineffective against (CW) continuous wave interference which may capture the receiver and therby actually degrade the performance.

The 50 Hz harmonic noise effects may be reduced by judicious choice of frequency by narrowband rejection filters and by using sophisticated rejection circuits which reduce the harmonic content.

The variation of the vertical magnetic field strength of atmospheric noise at the mine site is not known. So atmospheric noise data has been taken from the CCIR report. A plot of atmospheric noise field versus the frequency has been shown in Fig. 1.4. On the same figure the measured power line harmonic levels are shown.

2.2 SIGNAL PROPAGATION

Formal expressions for electric and magnetic fields excited by a vertical magnetic dipole placed below the surface of a semiinfinite conducting half space have been given by Wait and Campbell [9] and Sinha and Bhattacharya [10]. The results of these expressions are plotted as a normalised frequency dependent attenuation factors. The G factor applies to the attenuation experienced by the vertical magnetic field (Hz) measured directly above a vertical magnetic transmitting dipole, separated by the indicated number of skin depths (δ). A skin depth is defined by

$$\delta = \frac{1}{(\pi f \mu \sigma)^{1/2}}$$

where

f = frequency in Hertz

μ = permeability in H/m

σ = conductivity of earth in mhos/m

The vertical component of the magnetic field at the surface is given by

$$|Hz| = \frac{INA|G|}{2\pi Z^3}$$

where

INA = Transmitting antenna magnetic moment

I = Loop current in Amperes

N = Number of turns in transmitting loop

A = Loop area in sq.m.

Z = Loop depth in m

The rapid decrease in $|G|$ with increasing frequency indicates the large attenuation that signals above the VLF band incur in propagating through the earth. A plot of $|G|$ vs Z/δ has been shown in Fig. 2.1.

2.3 SIGNAL LEVEL AVAILABLE

The samples of the noise environment in which EM mine communication systems must operate has been discussed in Section 2.1. The performance of any data and voice communication system is ultimately limited by the signal-to- noise

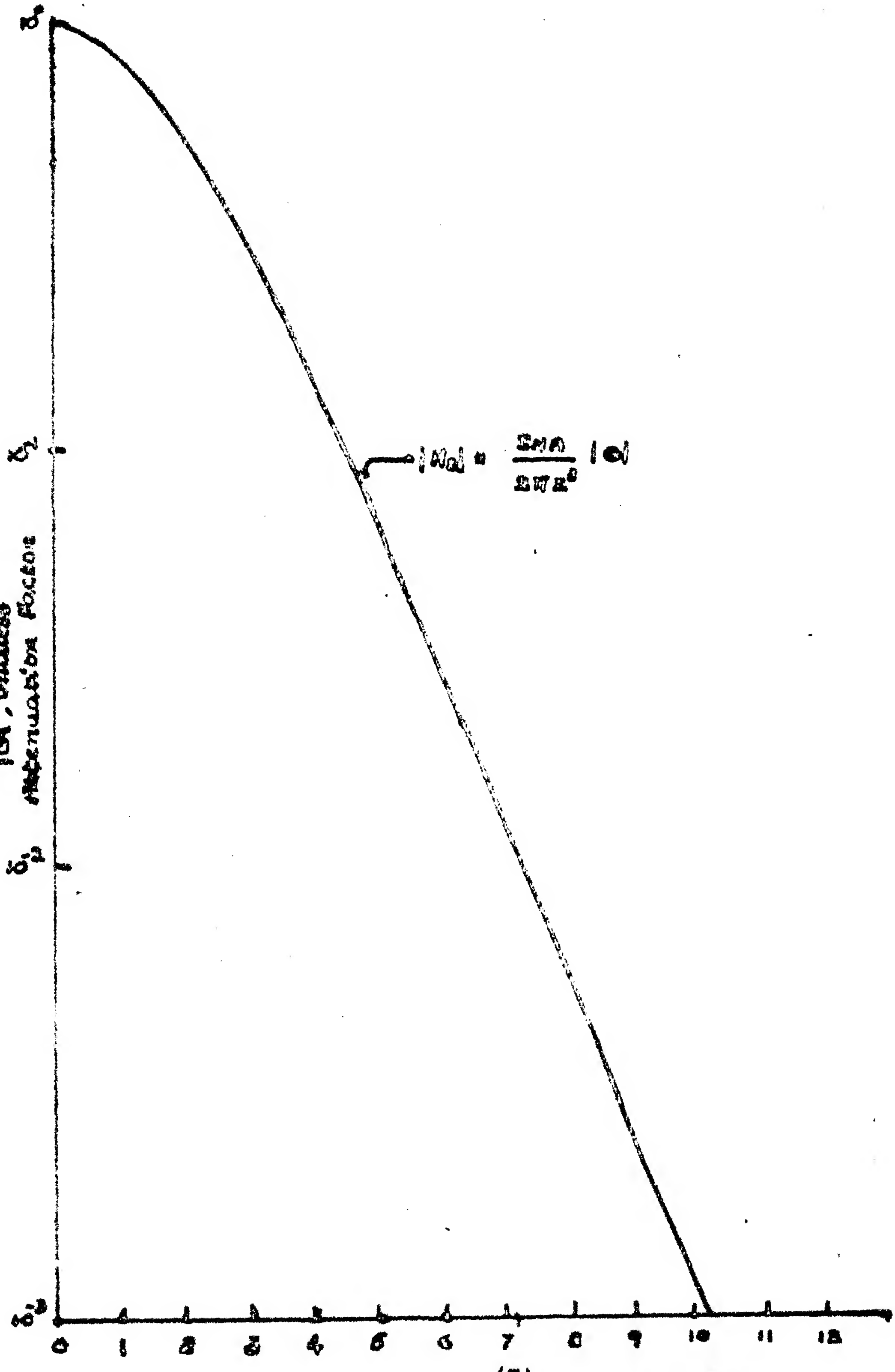

FIG. 2 PENETRATION INTO MEDIUM $\left(\frac{Z}{\delta}\right)$ in SKIN DEPTHS

ratio (S/N) available at the receiver. So the design parameters are to be so selected that the signal available at the receiver equals or exceeds that required to achieve a reliable transfer of information in a given noise environment.

A plot of signal amplitude at the surface versus the frequency has been shown in Fig. 2.2 for average earth conductivity. ~~On the same plot~~ the atmospheric noise level and power line harmonic interference levels are shown in Fig 1.4

2.4 SIGNAL-TO-NOISE RATIO REQUIRED FOR VOICE SYSTEMS

Available S/N depends on design parameters such as frequency bandwidth, path length, path conductivity, transmitter power and antenna configuration, whereas required S/N depends on signal design, data rate, signalling rate, modulation, detection, signal processing and reliability. The S/N available must equal or exceed the S/N required in order for the link to be usable.

Conventional voice channels operating with a 2.5 kHz bandwidth in a Gaussian noise environment require that the signal power be about 16 times the noise power i.e., S/N $\approx$ 12 dB. It is useful to show the input power requirements in different types of systems which will produce the required S/N. For comparison purposes it is assumed that the noise is Gaussian and N_o is the noise power spectral density in the RF bandwidth. B is the base bandwidth of the voice modulation

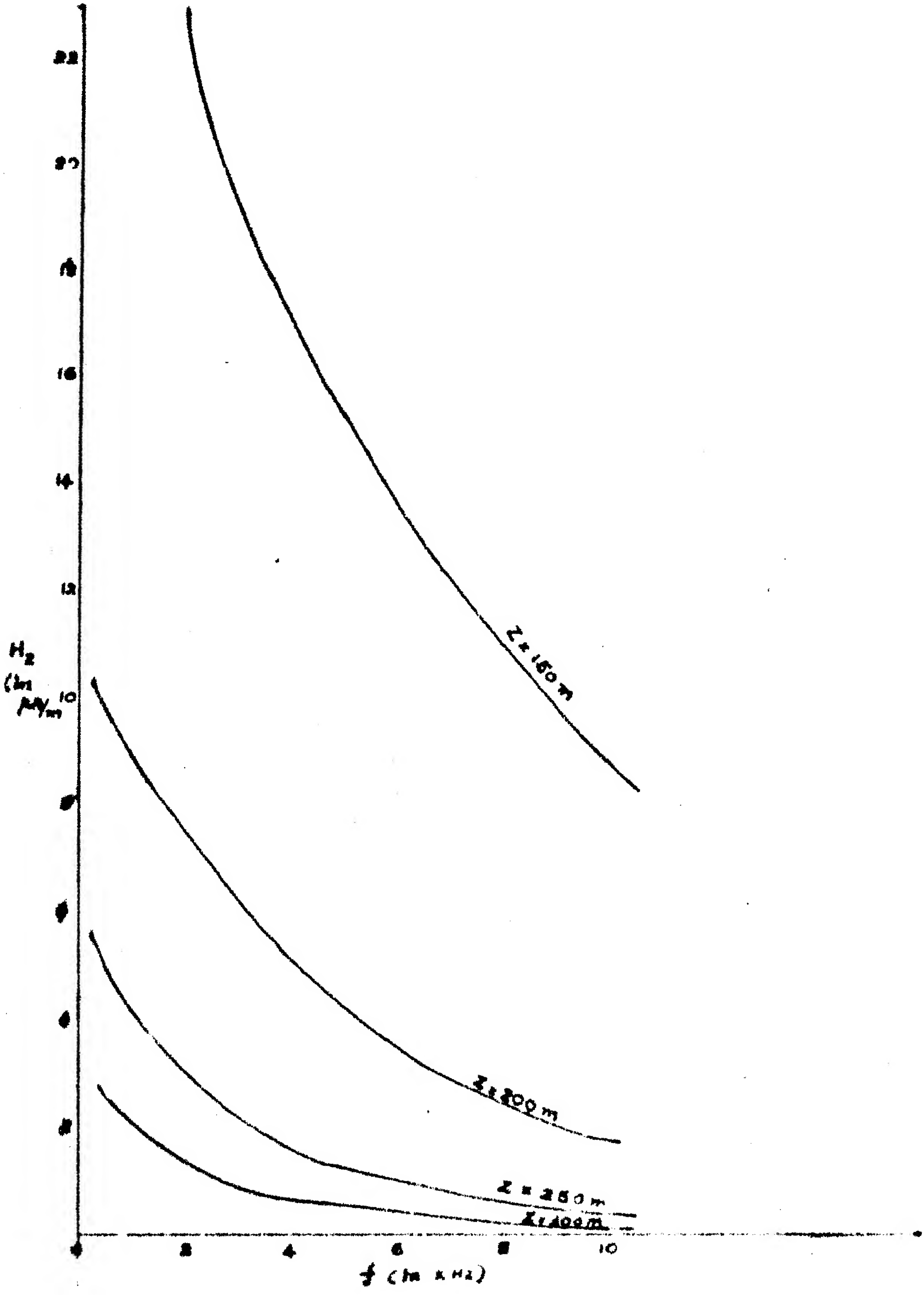

22
20
18
16
14
12
H_z (in $\mu V/m$)
10
8
6
4
2
0
2
4
6
8
10
f (in KHz)
Z = 150 m
Z = 200 m
Z = 250 m
Z = 400 m

... FREQUENCY

signal. The values of the received power input required are obtained assuming S/N = 10.

2.4.1 Direct Audio (available)

In this system no carrier modulation is required. The signal power equals the received power and the transmission bandwidth equals the signal bandwidth.

$$S/N = \frac{P_r}{N_i B}$$

$$P_r = 10\ N_o B$$

2.4.2 Amplitude Modulation Double Sideband width Envelope Detector

The received power is given by

$$P = P_c(1 + \frac{m^2}{2})$$

where m is the modulation index

P_c is the carrier power .

The rf bandwidth $B_{rf} = 2B$

Therefore, $S/N = \dfrac{\frac{m^2 P_r}{2}}{(1+\frac{m^2}{2})2BN_o}$

As speech can be clipped to one quarter of its amplitude with little effect on intelligibility, m = 0.5 can be taken for acceptable voice communication.

Therefore, $$10 = \frac{.5^2 \; P_r}{(1 + \frac{.5^2}{2}) \; 2BN_o}$$

or

$$P_r = 90 \; N_oB \; .$$

2.4.3 Amplitude Modulation - Double Sideband - Suppressed Carrier with Coherent Detection

$$S/N = \frac{P_r}{N_oB}$$

or

$$P_r = 10 \; N_oB$$

2.4.4 Amplitude Modulation - Single Sideband with Coherent Detection

$$P_r = 10 \; N_oB$$

2.4.5 Frequency Modulation

For FM

$$S/N = \frac{3}{2} \beta^2 \; \frac{P_r}{N_iB}$$

where β is modulation index.

For wideband FM with $m_f = 10$,

$$P_r = \frac{10 \times 2N_oB}{3 \times 10^2}$$

$$= .067 N_oB$$

For narrowband FM ($m_f = .5$)

$$P_r = \frac{10 \times 2N_oB}{3\times .5^2}$$

$$= 26.67\ N_oB$$

The results shown assume that the noise environment is Gaussian. In other types of noise the results may be quite different because the S/N required will be different. A table of the power requirements for voice systems has been shown.

Wideband FM which appear to be optimum on the basis of received power requirements is incompatible for through the earth mine communication systems because of the large bandwidth required ($\approx$ 60 kHz). AM Direct audio and AMSSB both appear to be optimum for through the earth systems in terms of received power and bandwidth requirements. But they are susceptible to impulse type noise.

AM Direct audio is most susceptible to manmade noise and interference which is prevalent at the lower audio frequencies.

The AMSSB systems can be made to operate above the frequencies where manmade noise and interference are most prevalent; however, these systems require more complex equipment for signal generation and detection. As can be seen from the expressions the transmitter power required for voice uplinks are high.

TABLE

SYSTEM	RECEIVED POWER REQUIREMENTS	BANDWIDTH REQUIREMENTS
AM DIRECT AUDIO	$10 N_o B$	B
AMDSB	$90 N_o B$	$2B$ ($m = \cdot 5$)
AMDSB - SC	$10 N_o B$	$2B$
AMSSB	$10 N_o B$	B
WBFM	$\cdot 067 N_o B$	$2 m_f B$ ($m_f = 10$)
NBFM	$26 \cdot 67 N_o B$	$2B$ ($m_f = \cdot 5$)

2.5 SIGNAL-TO-NOISE RATIO REQUIRED FOR DIGITAL DATA SYSTEMS

The E_b/N_o required for some binary modulation/demodulation systems operating in Gaussian noise has been taken from Haykins [11]. These curves are different when the systems are operated in non-Gaussian noise when atmospheric noise is clipped in bandwidth which are wide compared to signal bandwidth the E/N required may be several dB less than that required in Gaussian noise. Wideband clipping is not useful when inband interference is present which may capture the receiver.

2.5.1 Noncoherent FSK System

The coherent systems require added sophistication in the receiver to achieve improved performance. Hence noncoherent FSK scheme can be selected.

Assuming noise at the surface Gaussian, for bit error probability of in 10,000, the E_b/N_o required is given by

$$E_b/N_o = 12.5 \text{ dB}$$

Therefore, required $S/N_o = (E_b/N_o) \times (1/T) = \frac{E_b R}{N_o}$

$$(S/N_o)_{dB} = (E_b/N_o)_{dB} + 10 \log 12$$

$$= 23.29 \text{ dB}$$

N_o = Noise power spectral density measured in 1 Hz B.W.

Bandwidth of the system = 24 Hz

(S/N) required in 24 Hz bandwidth

$$S/N = (S/N_o) - 10 \log B$$

$$= 23.29 - 10 \log 24$$

$$= 9.4878876$$

Atmospheric Noise level at 2.5 kHz in 24 Hz B.W.

$$= N_o \times \sqrt{24}$$

$$= 3.3394\text{x}10^{-8} \sqrt{24}$$

$$= 1.63596\text{x}10^{-7} \text{ A/m}$$

$$= -135.72 \text{ dB relative to IA/m}$$

Therefore, the received signal level required

$$= 9.4878876 - 135.72$$

$$= -126.2366 \text{ dB rel 1 A/m}$$

$$= 4.87716\text{x}10^{-7} \text{ A/m}$$

The signal level available for a depth of 300 m is

$$Hz = \frac{INA}{2\pi z^3} \times |G| \qquad INA = 625 \text{ as per specification}$$

$$= \frac{625\text{x}.32}{2\pi\text{x}300^3}$$

$$= 1.17892\text{x}10^{-6} \text{ A/m}$$

For FSK the mark and space frequency arc so chosen that the they fall in between the power line harmonics. The frequency instability of power line frequency causes some harmonics to fall in band.

If the carrier frequencies arc 2475 Hz and 2525 Hz, the inband interference level may be of the order of 1.5 μA/m which is higher than the signal level for 300 m depth. So for noncoherent FSK scheme there will be implementation problems.

2.6 SIGNAL-TO-NOISE RATIO AVAILABLE AND REQUIRED FOR THE PROPOSED DIRECT SEQUENCE SPREAD SPECTRUM SYSTEM

Assuming the atmospheric noise at the surface as white Gaussian over the band of interest and spread spectrum eliminates the effect of power line interference, for coherent PSK for bit error ratio of 1 in 10^4,

$$E_b/N_o = 8 \text{ dB}$$

With data rate of 12 b/s and code length of 15

$$\begin{aligned}(S/N_o)_{dB} &= (E_b/N_o)_{dB} + 10 \log R \\ &= 8 + 10 \log 180 \\ &= 30.55 \text{ dB}\end{aligned}$$

B.W. of the system = 360 Hz

(S/N) required in 360 Hz bandwidth

$$S/N = (S/N_o) - 10 \log B$$

$$= 18.79 - 10 \log 360$$

$$= 4.98 \text{ dB}$$

Atmospheric noise level at 2.5 kHz in 24 Hz bandwidth

$$= 3.3394\text{x}10^{-8} \text{ x } \sqrt{24}$$

$$= 1.635\text{x}10^{-7} = -135.72 \text{ dB relative to 1A/m}$$

Therefore, the received signal level required

$$= 4.98-135.72 = -130.74 \text{ dB}$$

$$= 2.90\text{x}10^{-7} \text{ A/m}$$

The calculated value signal level available at 300 m depth for 10^{-2} conductivity and 625 A-T m^2, Hz = $1.17892\text{x}10^{-6}$ A/m

Because of the despreading capability of SS the power harmonic interference level is less compared to FSK case.

2.6.1 Atmospheric Noise Model for Non-Gaussian Case

Armospheric Noise model for non-Gaussian case has been taken from Swaft and Omura paper [12].

It is modelled as a narrowband process with a lognormal envelope with the form

$$a(t) = A\, e^{n(t)} \cos[\omega_c t+\Theta(t)]$$

where n(t) is a real stationary Gaussian process with zero-mean and autocorrelation given by

$$R_n(\tau) = \overline{n(t)\ n(t+\tau)}$$

A is a constant to be determined from noise power estimates, and and $\Theta(t)$ is a random phase process independent of the Gaussian process n(t) and is assumed to have uniform probability over o to 2π

$$P_\Theta(\alpha) = \begin{cases} 1/2\pi & o \leq \alpha \leq 2\pi \\ o & \text{otherwise} \end{cases}$$

The parameter V_d [Voltage deviation ratio] for Indian mines has been taken from the paper by Maxwell [13].

For PSK

E_b/N_o can be written as

$$E_b/N_o = \frac{P_s T}{(W)(\frac{A^2}{2}\ e^{2\sigma_n^2})}$$

where σ_n^2 is the variance of n(t) .

The total binary error probability for coherent binary PSK with integration time T smaller than the noise correlation time is given by

$$P_e = \frac{1}{2\pi} \int_o^\pi \phi \left[\frac{\log_e (\frac{\sqrt{2P}}{A\ \sin\Theta})}{\sqrt{\sigma_n^2}}\right] d\Theta$$

where $\phi(x) = \frac{1}{\sqrt{2\pi}} \int_x^\infty \exp(-1/2\ t^2)\ dt$

and $V_d = 20 \log \left(\frac{E_{rms}}{E_{av}}\right)$. Taking the value of V_d to be 9 we get

$$10\ \sigma_n^2 \log_{10}^e = 9$$

$$\sigma_n^2 = \frac{9}{10 \log_{10} e}$$

$$\sigma_n = 1.43955$$

$$N_o W = \frac{A^2}{2} e^{2\sigma_n^2}$$

or

$$A^2 = \frac{2N_o W}{e^{2\sigma_n^2}}$$

$$A = 2.06 \times 10^{-4} \quad \text{for 15 bit code length}$$

2.7 ERROR PROBABILITY DERIVATION FOR DSSS

The transmitted signal is given by

$$S(t) = P_s\ b(t)\ a(t)\ \cos \omega_c t$$

where

$b(t)$ = data sequence

$a(t)$ = SS code sequence

P_s = signal amplitude

f_c = carrier frequency.

The received signal is

$$r(t) = S(t) + n_a(t) + \sum_{n=1}^{K} A_n \cos(\omega_n t + \phi_n)$$

where $n_a(t)$ = atmospheric noise

$$\sum_{n=1}^{K} A_n \cos(\omega_n t+\phi_n) = \text{Power line harmonic interference}$$

(Power line harmonic interference is deterministic but not known).

Suppose the symbol 1 was transmitted

$$H_1 : \quad \mathcal{L} = \int_0^T S(t)\, a(t) \cos \omega_c t\, dt$$

$$+ \int_0^T n_a(t)\, a(t) \cos \omega_c t\, dt$$

$$+ \sum_{n=1}^{K} \int_0^T A_n \cos(\omega_n t+\phi_n)\, a(t) \cos \omega_c t\, dt$$

$$= \mathcal{L}_1+\mathcal{L}_2+\mathcal{L}_3$$

$$E[L_1] = \int_0^T E[P_s\, a^2(t) \cos^2 \omega_c t]\, dt$$

$$= \frac{P_s T}{2}$$

$$E[L_2] = 0$$

$$E[L_3] = \int_0^T E[A_n \cos(\omega_n t+\phi_n)\, a(t) \cos \omega_c t]\, dt$$

$$= \int_0^T \frac{A_n}{2} \cos[(\omega_c-\omega_n)t-\phi_n]\, a(t)\, dt$$

At $\omega_c = \omega_n$

$$E[L_3] = \frac{A_n T}{2N} \cos\phi_n$$

Sum term $\omega_c+\omega_n$ will make very little contribution.

At $\omega_c \neq \omega_n$

$$E[L_3] = \frac{A_n}{2} \int_0^T \cos[(\omega_c-\omega_n)t - \phi_n]\, a(t)\, dt$$

$$\simeq \frac{A_n}{2N} \left[\frac{\sin(\overline{\omega_c-\omega_n}T - \phi_n)}{\omega_c-\omega_n} - \frac{\sin \phi_n}{\omega_c-\omega_n} \right]$$

Due to $\omega_c-\omega_n$ in the denomination all other harmonics will contribute less

$$Var[L/H_1] = \sigma_1^2 = E[\ L-E[L/H_L]\ ^2]$$

$$= E[L^2/H_1] - \ E[L/H_1]^2$$

$$= \int_0^T \int_0^T E[n_a(t_1)n_a(t_2) \cos \omega_c t_1 \cos \omega_c t_2 \; a(t_1)\, a(t_2)]\, dt_1\, dt_2$$

$$= \int_0^T \int_0^T E[n_a(t_1)n_a(t_2)]\, E[a(t_1)\, a(t_2)$$

$$= \frac{N_o}{2} \int_0^T \int_0^T \delta\,(t_1-t_2)\; E[a(t_1)\, a(t_2) \; \cos\omega_c t_1 \cos\omega_c t_2] dt_1 dt_2$$

[Assuming $n_a(t)$ as white Gaussian Noise]

$$= \frac{N_o}{2} \int_0^T E[a^2(t) \cos^2 \omega_c t]\, dt$$

$$= \frac{N_o}{2} \frac{T}{2} = \frac{N_o T}{4}$$

$$m_1 = E[L_1] + E[L_3)] \qquad E[L_2] = 0$$

$$= \frac{P_s T}{2} + \frac{A_n T}{2N} \cos \emptyset_n$$

Putting $\emptyset_n = 0$ (worse case)

$$m_1 = \frac{T}{2} [P_s + \frac{A_n}{N}]$$

Suppose the symbol 0 was transmitted. On doing similar analysis

$$m_o = \frac{T}{2} [-P_s + \frac{A_n}{N}]$$

$$\sigma_o^2 = \frac{N_o T}{4}$$

Error probability $P_e = P_o P_F + P_1 P_M$

$$= 1/2\ (P_F + P_M)$$

where P_F = Probability of false alarm

$$= \int_r^\infty N[m_o, \sigma_o^2]\, dx = \int_r^\infty p_{x/H_o} (x|_{H_o})\, dx$$

P_M = Probability of false dismissal

$$= \int_{-\infty}^r N[m_1, \sigma_1^2]\, dx = \int_{-\infty}^r p_{x|H_1} (x|H_1)\, dx$$

The threshold γ is set as zero

$$\text{Therefore, } P_e = \frac{1}{2}\left[\int_0^{\infty} e^{-(x+m_o)^2/2\sigma_o^2}\,dx\right.$$

$$\left.+\int_{-\infty}^{0} e^{-(x-m_1)^2/2\sigma_1^2}\,dx\right]$$

$$= \frac{1}{2}\left[\operatorname{erfc}\left(\frac{m_o}{\sigma_o}\right) + \operatorname{erfc}\left(\frac{m_1}{\sigma_1}\right)\right]$$

{The theoretical results are shown from Figs. 2.3 to 2.7}. The optimum frequency is chosen to be 2.5 kHz as there is a deep notch in atmospheric noise level around 2-3 kHz that can be seen in Fig. 1.4. The error probability vs $\frac{E_b}{N_o}$ ~~are~~ is shown in ~~Figs.~~ Fig. 2.4.

2.8 ERROR PROBABILITY DERIVATION FOR THE SYSTEM CONSTRUCTED

Received signal

$$r(t) = S(t) + n_a(t) + \sum_{n=1}^{K} A_n \cos(\omega_n t+\emptyset_n)$$

Suppose symbol 1 was transmitted. $T = T_a$ = Chip Interval

$$H_1:1 = \int_0^T r(t)\cos\omega_c t = \int_0^T S(t)\cos\omega_c t + \int_0^T n_a(t)\cos\omega_c t\,dt$$

$$+ \sum_{n=1}^{K}\int_0^T A_n \cos(\omega_n t+\emptyset_n)\cos\omega_c t\,dt$$

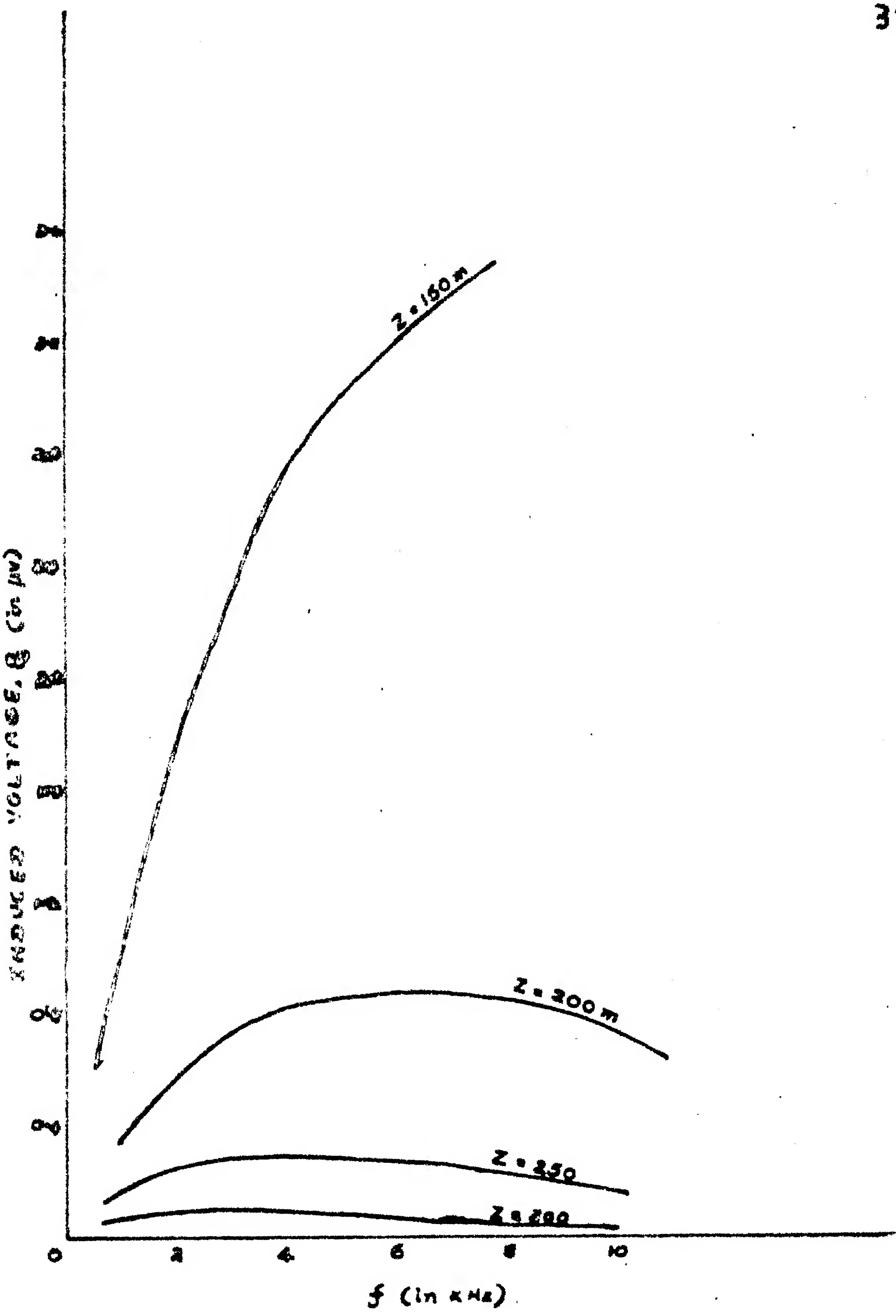

FIG 3.3 SIGNAL AMPLITUDE VS FREQUENCY

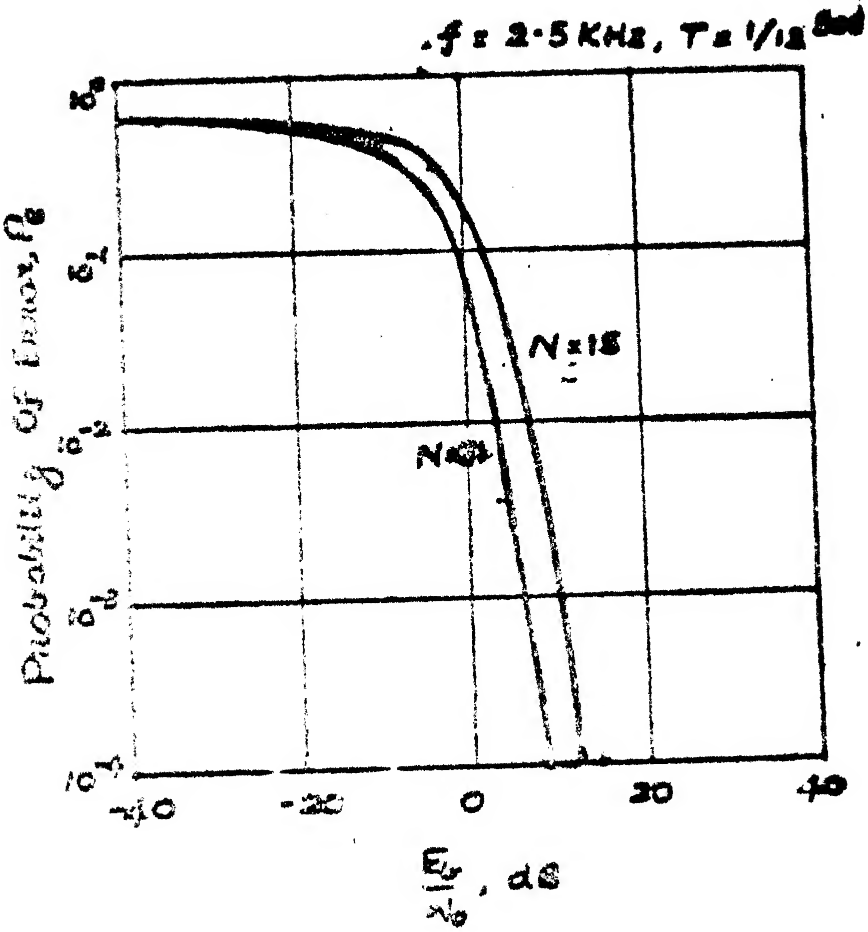

Fig. 3.4 Error Probability Vs $\frac{E_b}{N_0}$

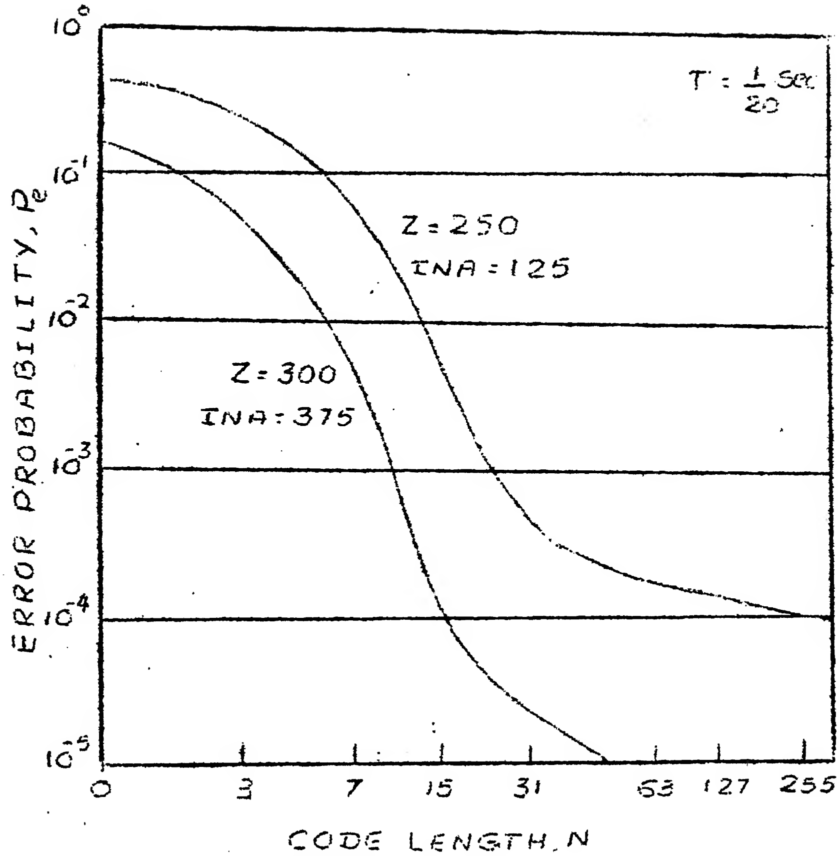

FIG 2.5 ERROR PROBABILITY Vs CODE LENGTH.

'N' CAN'T BE BEYOND 31 DUE TO CHANNEL/ANTENNA B.W. LIMITATION. FOR Z = 250, IT CAN BE SEEN 'N' BEYOND 127 DOESN'T OFFER MUCH IMPROVEMENT IN PERFORMANCE.

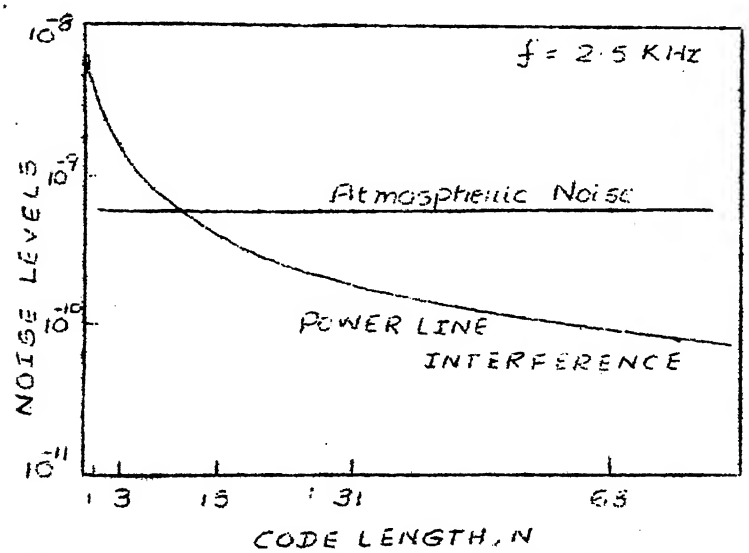

FIG 2.6 NOISE LEVEL Vs CODE LENGTH

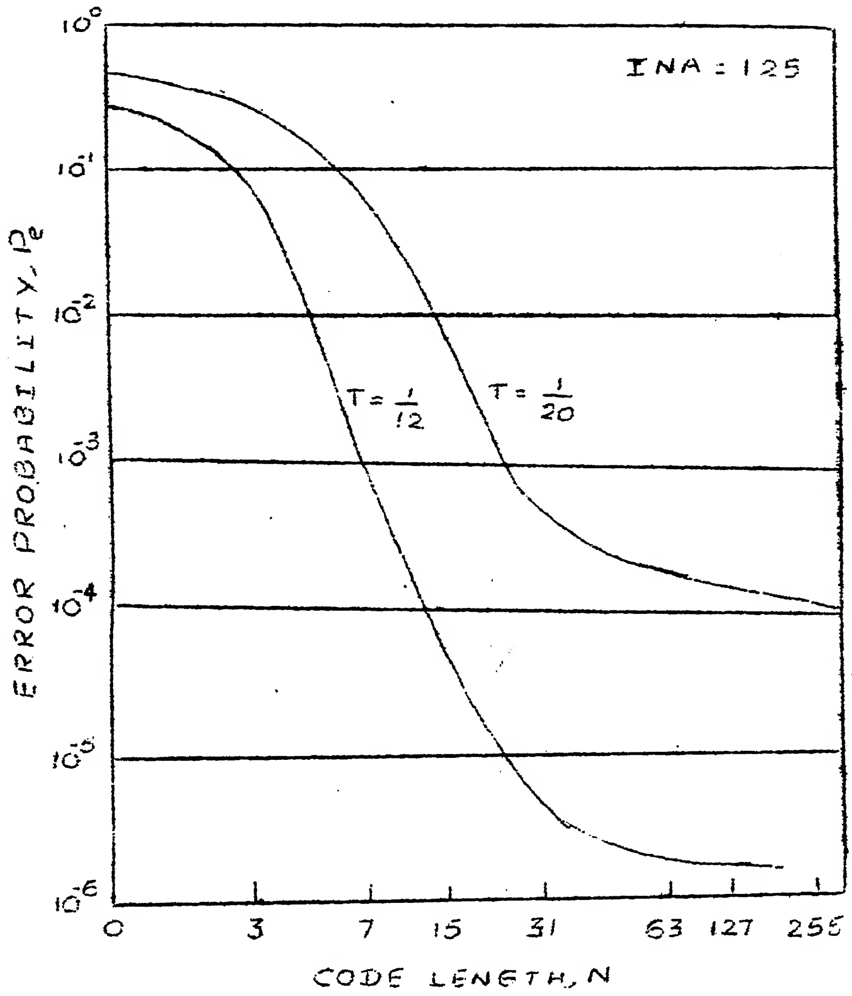

FIG 2.7 ERROR PROBABILITY VS CODE LENGTH.
IT CAN BE SEEN THE PERFORMANCE
DETERIORATION AS THE KEYING RATE
IS INCREASED.

Proceeding on similar lines as earlier

$$\int_0^T S(t)\cos\omega_c t\,dt = \frac{P_s T}{2}$$

$$\int_0^T A_n \cos(\omega_n t+\phi_n)\cos\omega_c t\,dt$$

$$= \frac{A_n}{2}\int_0^T \cos(\overline{\omega_c-\omega_n}t-\phi_n) \qquad (13)$$

($\omega_c+\omega_n$ term will contribute very small value)

$$= \frac{A_n}{2}\frac{\sin[\overline{\omega_c-\omega_n}T-\phi_n]}{\omega_c-\omega_n} + \frac{A_n \sin\phi_n}{2(\omega_c-\omega_n)}$$

At $\omega_c = \omega_n$, substituting in (13),

$$\int_0^T A_n \cos(\omega_n t+\phi_n)\cos\omega_c t\,dt = \frac{A_n T}{2}\cos\phi_n$$

Considering the worst case $\phi_n = 0$

$$m_1 = E[L/H_1] = \frac{P_s T}{2} + \frac{A_n T}{2}$$

$$\sigma_1^2 = \cancel{\frac{P_s T}{2}\left[\frac{N_o}{2} - \frac{A_n T}{2}\right]} = \frac{N_o T}{4}$$

$$m_o = -\frac{P_s T}{2} + \frac{A_n T}{2}$$

$$\sigma_o^2 = \cancel{\frac{P_s T}{2}\left[\frac{N_o}{2} + \frac{A_n T}{2}\right]} = \frac{N_o T}{4}$$

$$P_F = \frac{1}{2}\,\mathrm{erfc}\left(\frac{m_o}{\sigma_o}\right)$$

$$P_M = \frac{1}{2}\,\mathrm{erfc}\left(\frac{m_1}{\sigma_1}\right)$$

$$P_e = \frac{1}{2}(P_F + P_M)$$

The data bits are decided by putting a threshold on the digital magnitude comparator. Probability of making correct decision

$$= \cancel{\sum_{r=0}^{\frac{N-1}{2}} {}^{N}C_r \, P_F^r \, P_M^r} = \sum_{\pi=0}^{\frac{N-1}{2}} {}^{N}C_\pi \, P_e^{\pi} (1-P_e)^{N-\pi}$$

$$(N = 15)$$

Therefore, error probability in the demodulated data

$$= 1 - P_c = 1 - \sum_{\pi=0}^{\frac{N-1}{2}} {}^{N}C_\pi \, P_e^{\pi} (1-P_e)^{N-\pi}$$

$$\cancel{= 1 - \sum_{r=0}^{\frac{N-1}{2}} {}^{N}C_r \, P_F^r \, P_M^r}$$

2.9 OPTIMISATION OF OPERATING FREQUENCY; ~~AND~~ CODE LENGTH LIMITATIO

The information that may be of most value to communication system design is the signal amplitude variation between 2 kHz and 3 kHz where there is a variable but significant (> 10 dB) minimum in atmospheric noise. This deep notch is caused by the high attenuation of distant sources propagating in earth ionosphere waveguide. So an optimum frequency of 2.5 kHz is chosen which covers considerable depths.

As the atmospheric noise is assumed to be white Gaussian, over the band of interest, SS will neither improve nor deteriorate the performance as far as the atmospheric noise is concerned. A plot of noise level vs code length has been shown in Fig. 2.5.

CHAPTER 3

VLF TRANSMITTER

3.1 SCHEME

The data sequence which is in binary format is modulo-2 added to the code sequence and this in turn is used to modulate the carrier for PSK generation. The transmitter has been built for both asynchronous and synchronous transmissions.

The block diagram of the synchronous transmitter has been shown in Fig. 3.1. Here continuous data is added to Pseudo random binary sequence (PRBS) as shown in Fig. 3.1.

The block diagram of the asynchronous transmitter has been shown in Fig. 3.2. Here the serial data from the keyboard interface unit (KIU) is added to the spreading code.

The transmitter has been constructed to work from 3V as per specification using digital CMOS ICs.

3.2 CLOCK GENERATION UNIT (CGU)

The 180 Hz clock for the PRBS, 12 Hz clock for the parallel to serial data conversion, 2.5 kHz clock for the carrier generation are all derived from the clock generation unit (CGU). The CGU is shown in Fig. 3.3.

A crystal controlled clock generation though not employed in the system was also tried out. This is shown in Fig. 3.3.1.

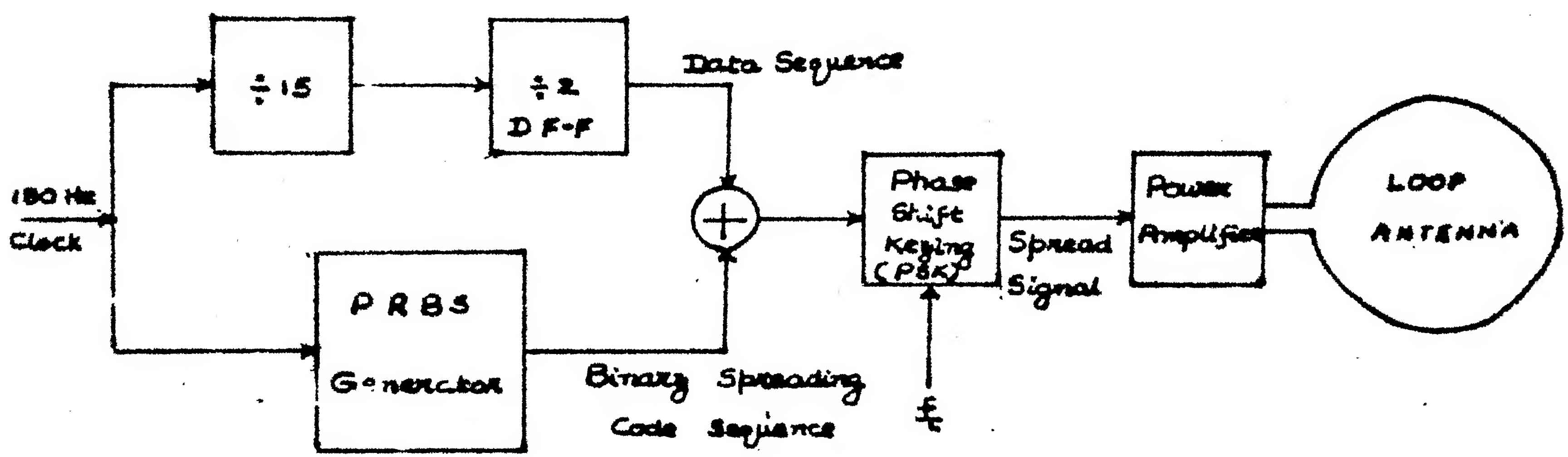

Fig 31 VLF TRANSMITTER (SYNCHRONOUS)

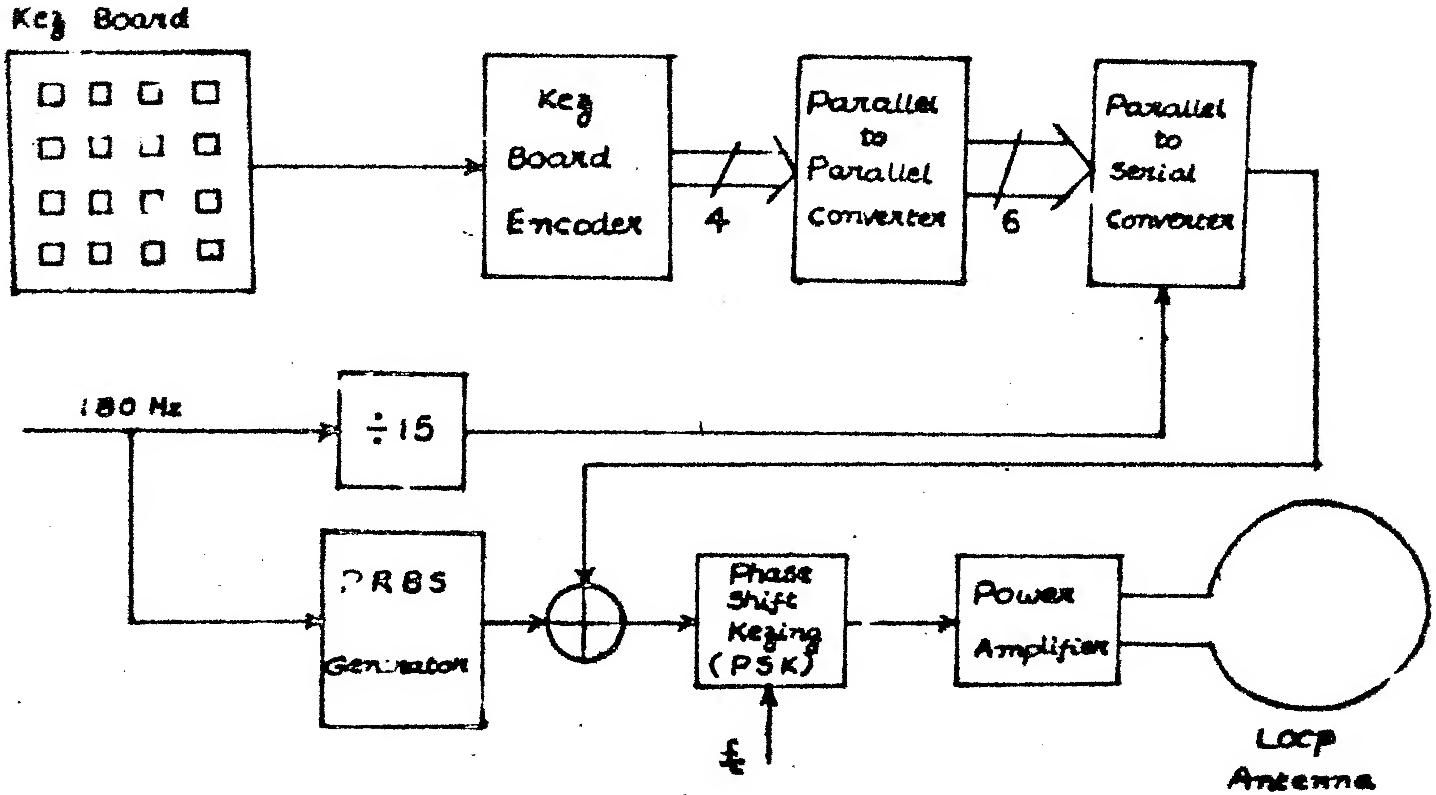

Fig. 3.2 Block Diagram Of the VLF Transmitter

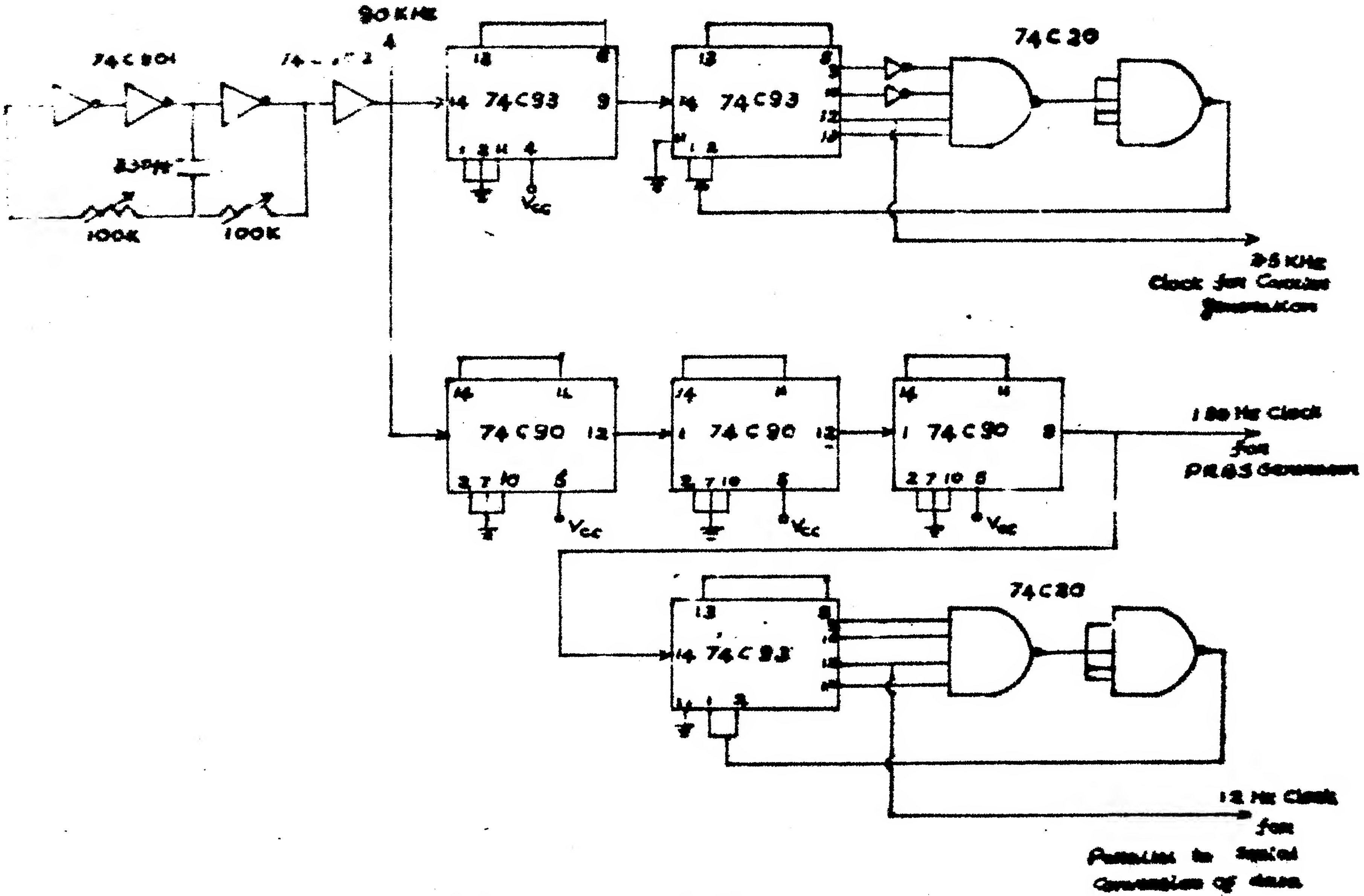

Fig 3.8 CLOCK GENERATION UNIT (CGU)

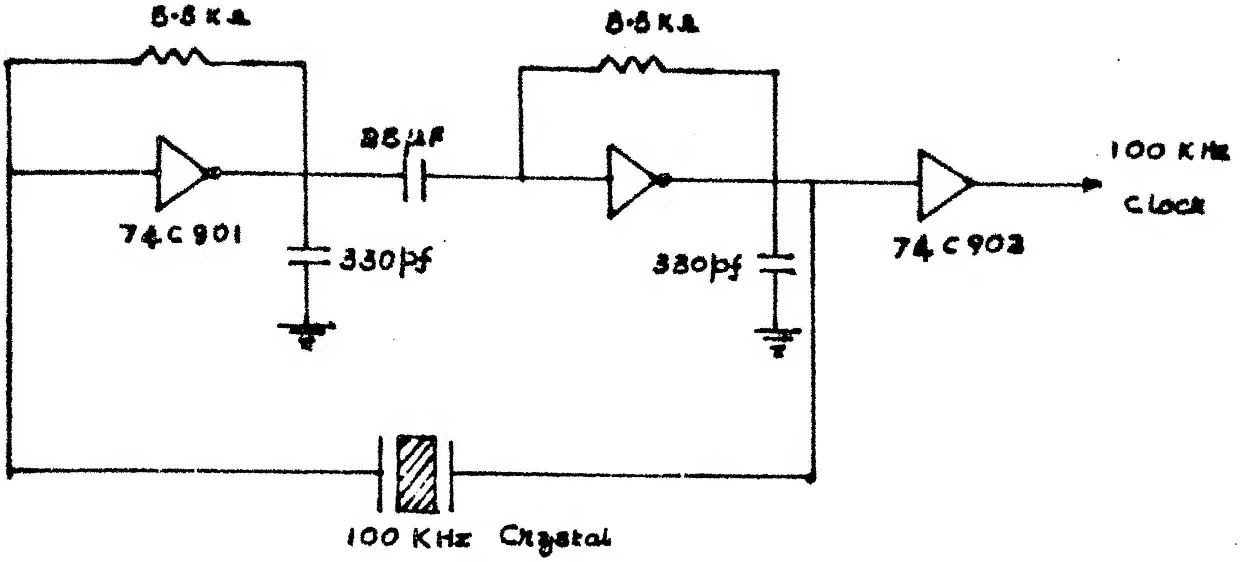

Fig 3.31 Crystal Clock Generation

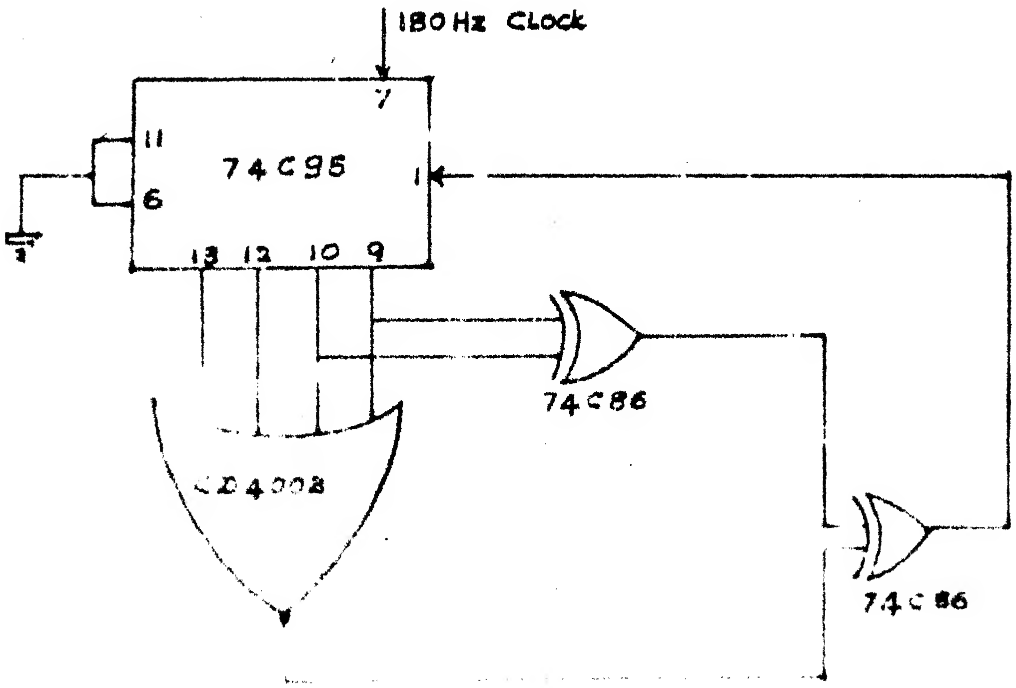

The PRBS clock can be generated from the data clock using (PLL) phase locked loop. But due to the nonavailability of PLLS which work at 3V this is not tried out.

3.3 PRBS GENERATION

A 4-bit shift register is used to generate a maximal linear code sequence of length 15. The tappings are taken from the third and fourth stages of the register. The feature to avoid the all zero state is provided. The PRBS generator is shown in Fig. 3.4.

3.4 PSK GENERATION

The PSK has been generated using passive low pass filters (LPFs),Transistor amplifiers and analog switches. The reason for using passive LPF is that OPAMPs which work at +3V as a LPF were not available. The modulated sequence is used to control the analog switches to generate the PSK. The circuit diagram is shown in Fig. 3.5.

A second method of generating PSK is shown in Fig. 3.6. This method actually involves generating the PSK at the digital level and filtering it to get the actual PSK. This method also works satisfactorily at +3V.

The usual methods of generating PSK using a modulator chip like XR-205 or analog multiplier chips like XR 2208, MC 1496 cannot be used here as these chips cannot work from a single +3V power supply.

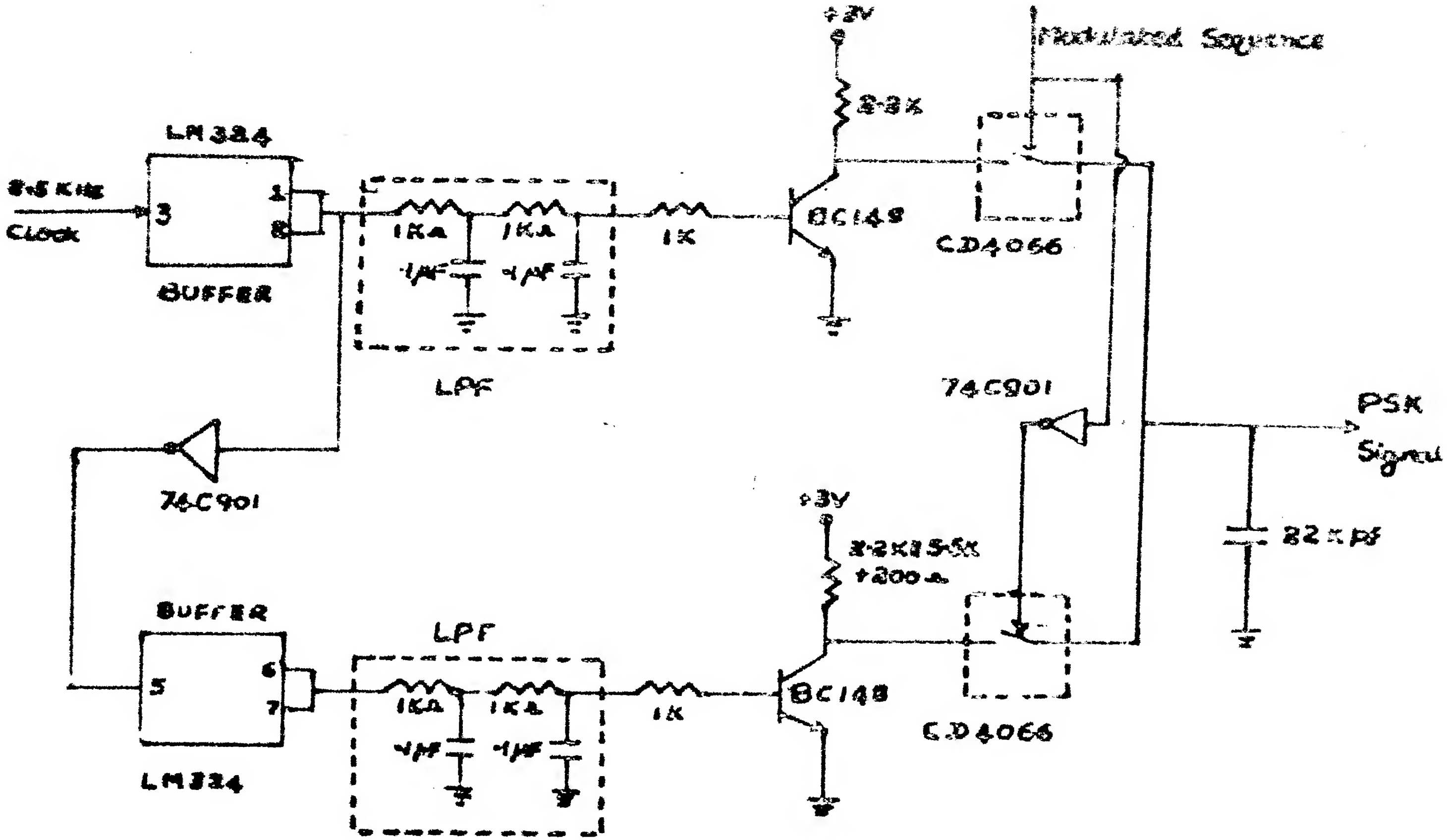

Fig 3.6 PSK GENERATION

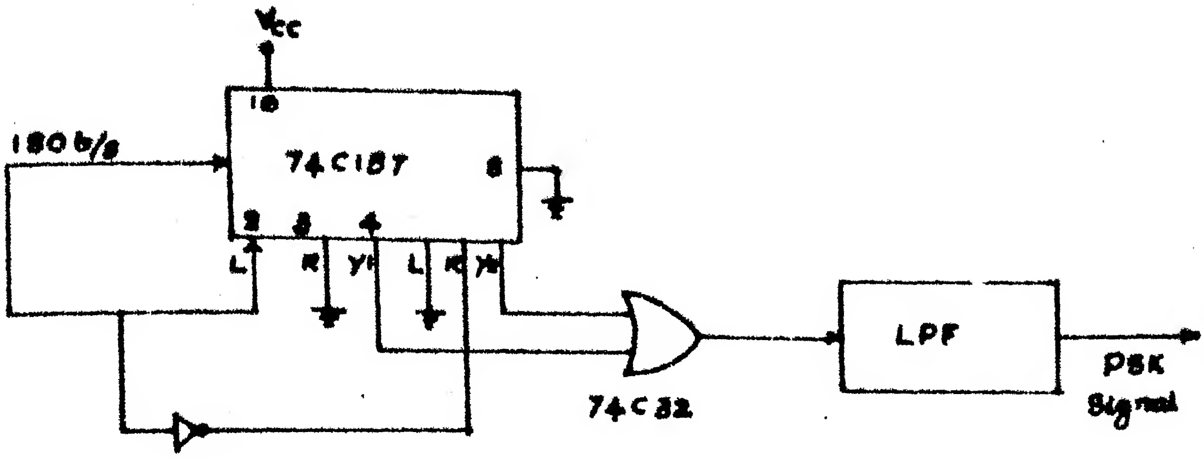

Fig 3·6 PSK GENERATION

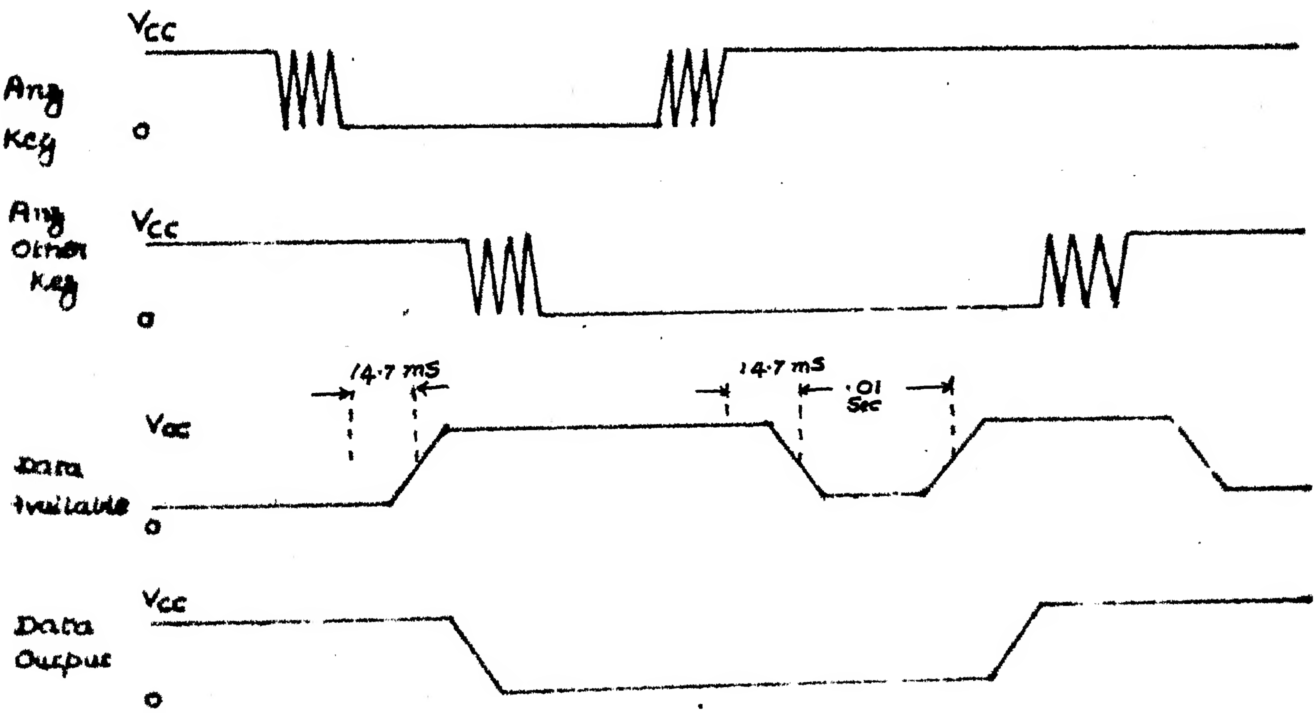

Fig 3·9 Timing waveforms of Keyboard Encoder

The full diagram of the synchronous transmitter has been shown in Fig. 3.7.

3.5 KEYBOARD INTERFACE UNIT (KIU)

The keyboard interface unit (designed) (to work at 3V) has been shown in Fig. 3.8.

The CMOS key encoder 74C922 provides all necessary logic to encode an array of switches. This is a 16 key encoder. The keyboard scan is implemented by using an external capacitor C_{DSC}. The debounce circuit needs only a single external capacitor C_{KBM}. The timing waveforms are shown in Fig. 3.9.

F_{SCAN} = keyboard scan rate

= 1 kHz

C_{OSC} = .06 μF from the CMOS data book for 1 kHz scan rate

The debounce period is chosen to be .01 sec.

$$0.7RC_{KBM} = .01$$

where R = internal resistance = 10 K Ohms

Therefore, $C_{KBM} = 1.47\ \mu F$

Once a key is pressed data available (DA) goes high indicating the acceptance of the key. The tristate control ($\overline{\text{output enable}}$) is now made low, for the 4 bit code corresponding to the key depressed to appear at the output pins. The ringing is avoided by using the Schmitt Triggers CD 40106. The

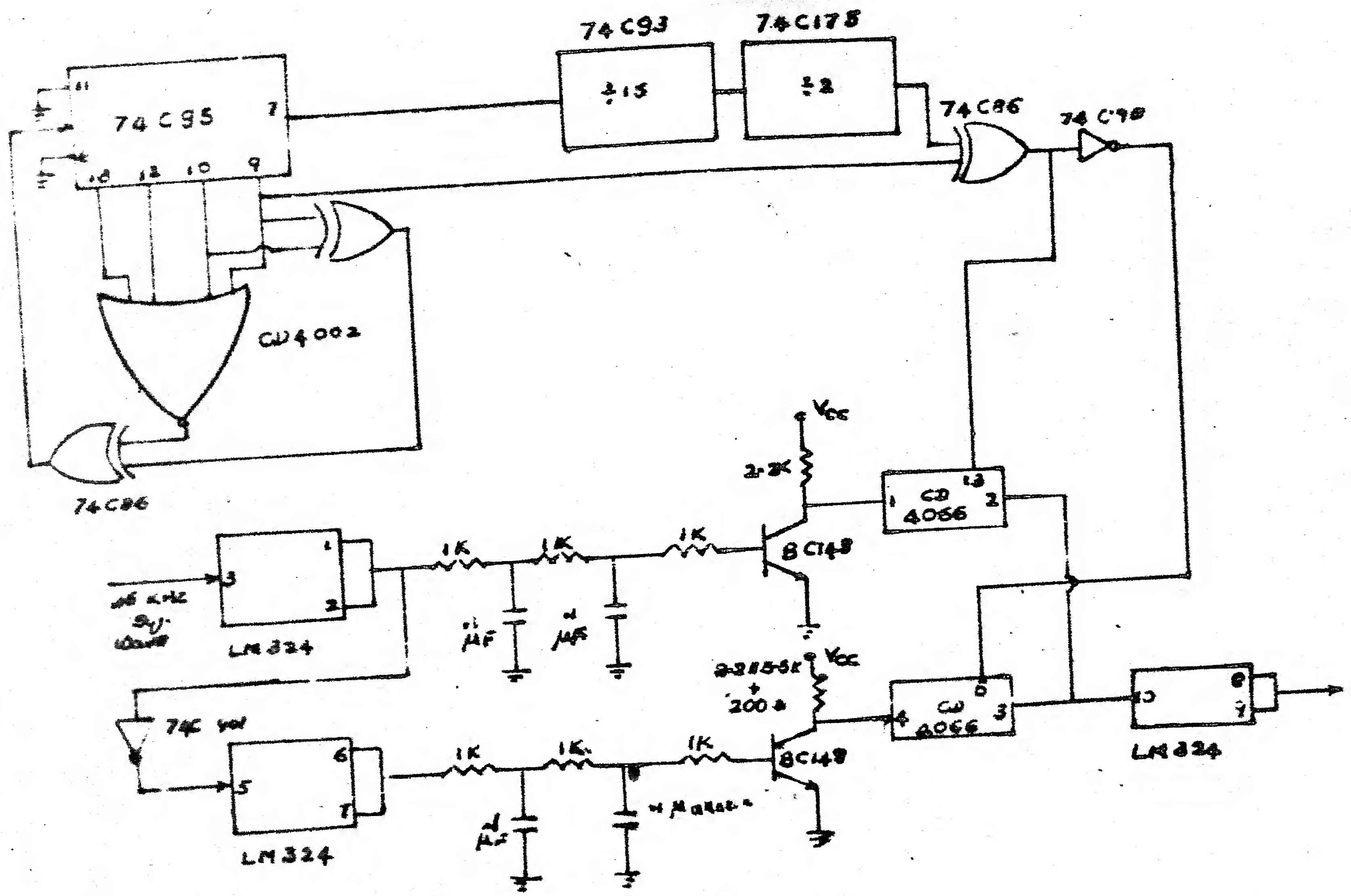

Fig 5·7 VLF TRANSMITTER (SYNCHRONOUS)

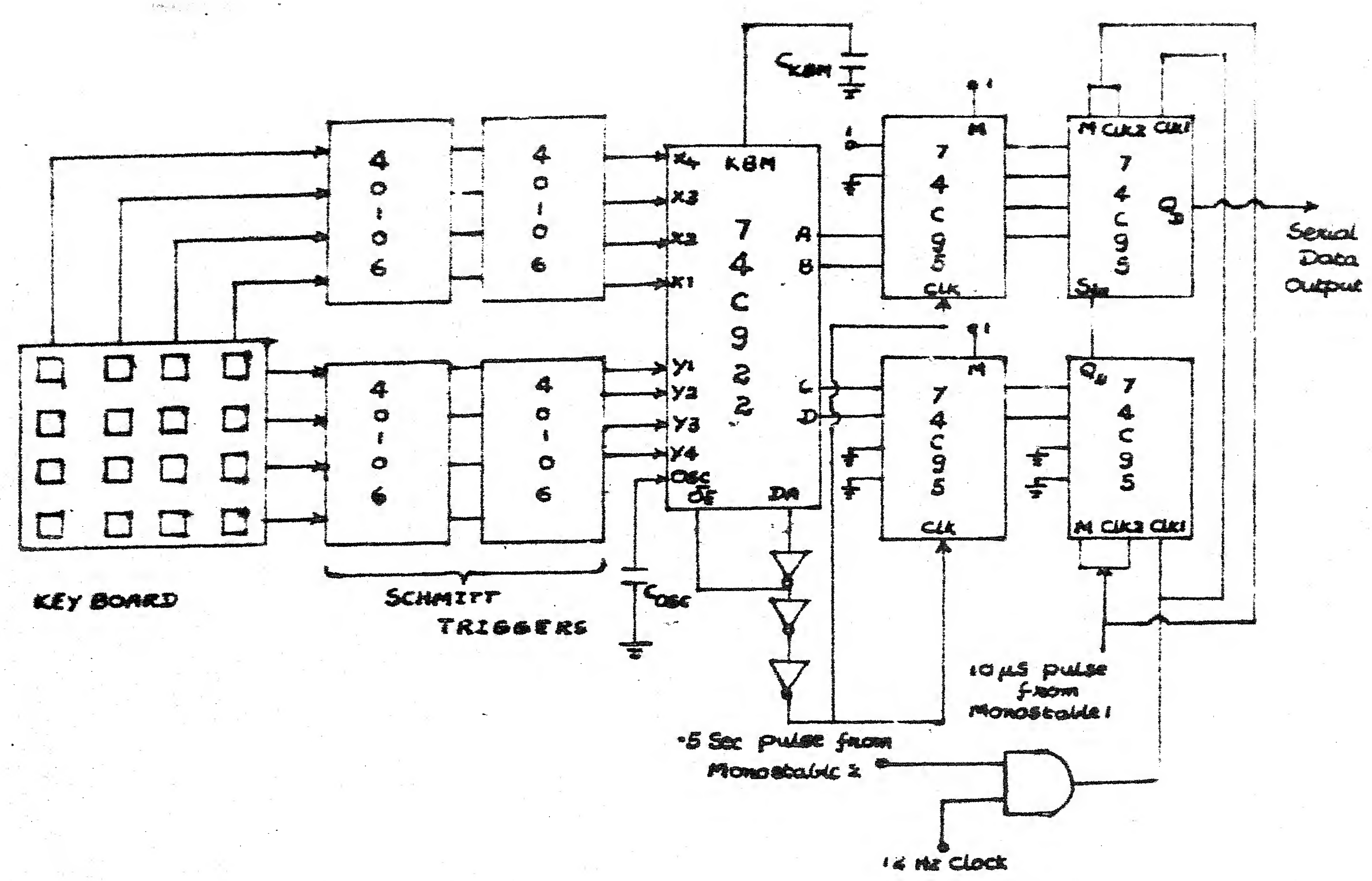

FIG 3-8 KEYBOARD INTERFACE UNIT

The 2-Key roll over of the keyboard encoder can be seen in Fig. 3.9.

The parallel to parallel converter is used to load the 6 bits 1,0 and the 4 bits code corresponding to the key. This parallel output is serially shifted out to the DF-F as shown in Fig. 3.8

When there is no transmission either 0 or the code sequence corresponding to 0 can be transmitted. By sending the code sequence, the receiver will be in lock condition so the initial acquisition for the receiver is not a problem. Unless 1 followed by 0 is there the message bits are not latched in. At the receiver the inverter output will be essentially zero when there is no transmission. The rising edge followed by the falling edge triggers the receiver and indicates that there is transmission.

The mode control and clock for the parallel to serial converter are given from two monostables. The low to high transition of DA triggers monostable 1. A narrow pulse of width 10 μs is used to load, the code corresponding to the key. This pulse is also used to trigger monostable 2. Monostable 2 generates a pulse of slightly greater than .5 sec. width which enables the 12 Hz clock over this period.

The complete diagram of the asynchronous transmitter has been shown in Fig. 3.10.

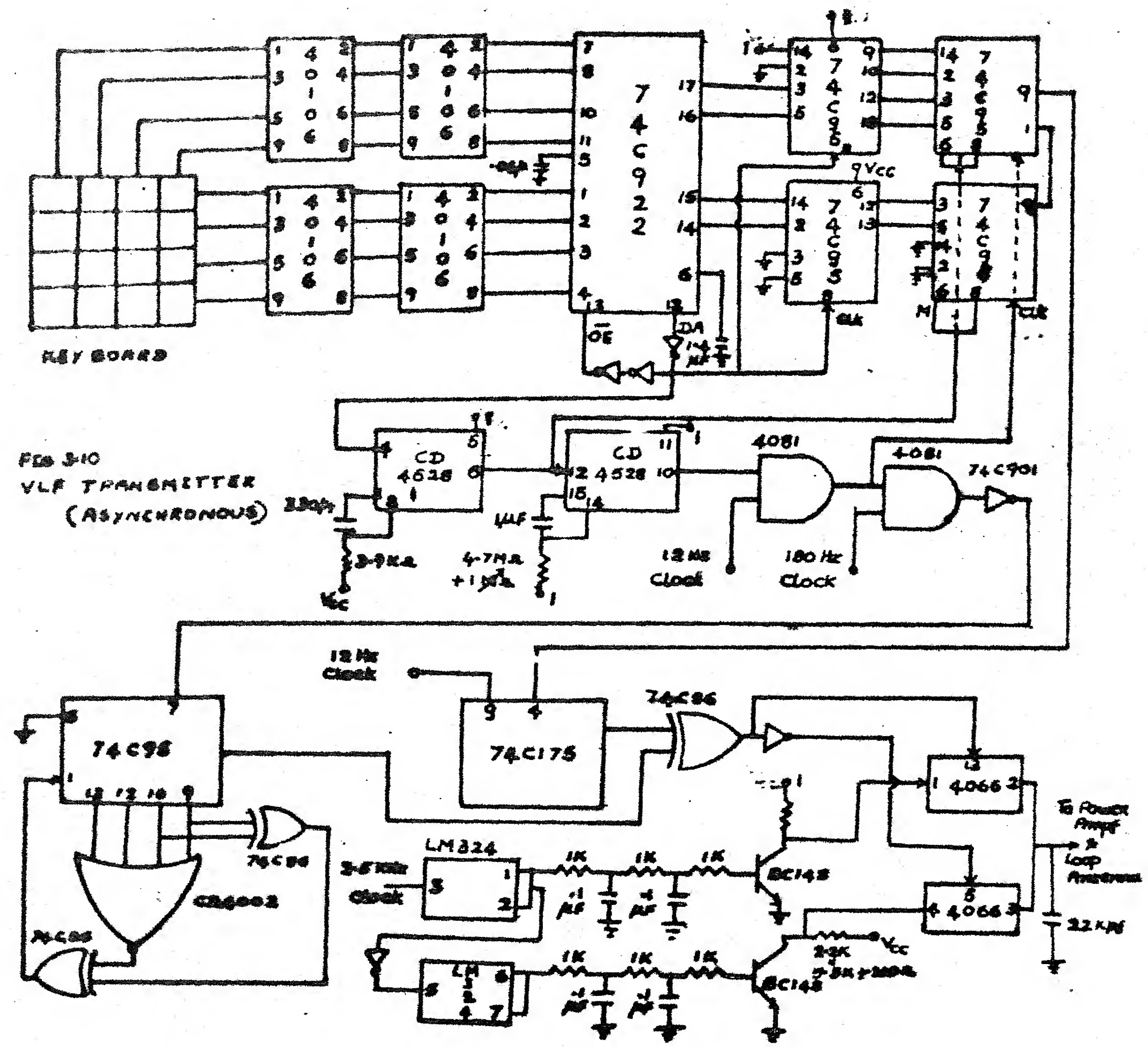

FIG 3-10
VLF TRANSMITTER
(ASYNCHRONOUS)

CHAPTER 4

VLF RECEIVER

4.1 SCHEME

The high noise level influences the design of the RF section in the communications receiver. The receiver design is somewhat more critical than the transmitter design mainly because of the presence of interfering signals before the signal processing stage. The RF section must discriminate against noise as much as possible and then amplify the modulated signal and noise in a linear way before the signal processing stage. Predetection filtering is useful in discriminating against noise that occurs outside the occupied bandwidth of the modulated signal.

The block diagram of the synchronous communication receiver has been shown in Fig. 4.1. The received signal is first amplified and then bandpass filtered to eliminate the power line harmonics and atmospheric noise out of band. The carrier is rec~~o~~overed using the squaring loop method. It is multiplied with the incoming modulated signal and the resulting signal is low pass filtered to get an approximate code sequence. A bit synchroniser is constructed for the clock recovery of the SS sequence. The bits are decided at the chip level first by integration and dumping and putting a threshold on the decision

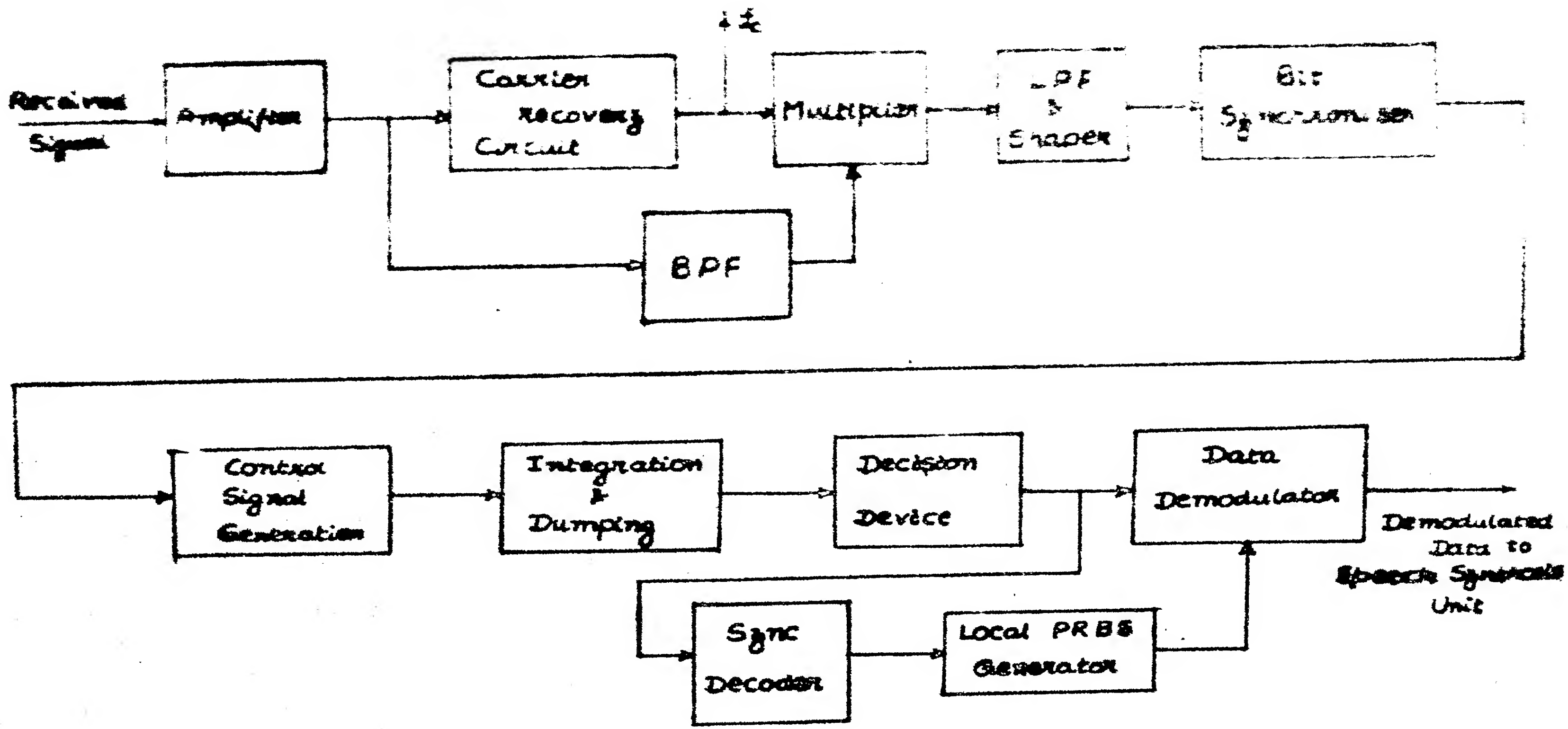

Fig 4.1 Block Diagram of the VLF Receiver

device. A replica of the transmitted SS code is generated at the receiver in synchronism with the received code sequence. The frame synchroniser generates a pulse at each frame of the incoming SS code sequence which sets the local PRBS generator. The data bits are decided by correlating with the local sequence.

4.2 COHERENT CARRIER RECOVERY

A block diagram of the carrier recovery by squaring loop method has been shown in Fig. 4.2.

A convenient and attractive way to derive the phase of the carrier reference is to make use of the squaring loop. The received signal is first bandpass filtered and squared to remove the modulation. The resultant double frequency term is then tracked by means of a phase locked loop whose VCO output is frequency divided by two and used as an estimate of the carrier reference. Performance of the squaring loop has been shown to be equivalent to that of costas loop although the 180° phase ambiguity introduced by having a twice frequency coherent reference must be resolved.

The circuit diagram of the coherent carriery is shown in Fig. 4.3. The 180° phase ambiguity is not resolved here. If the carriers are 180° out of phase then they brought back to in phase by manually resetting the D flip-flop. The XR 2208 multiplier chip is used here as squarer. It has a built-in

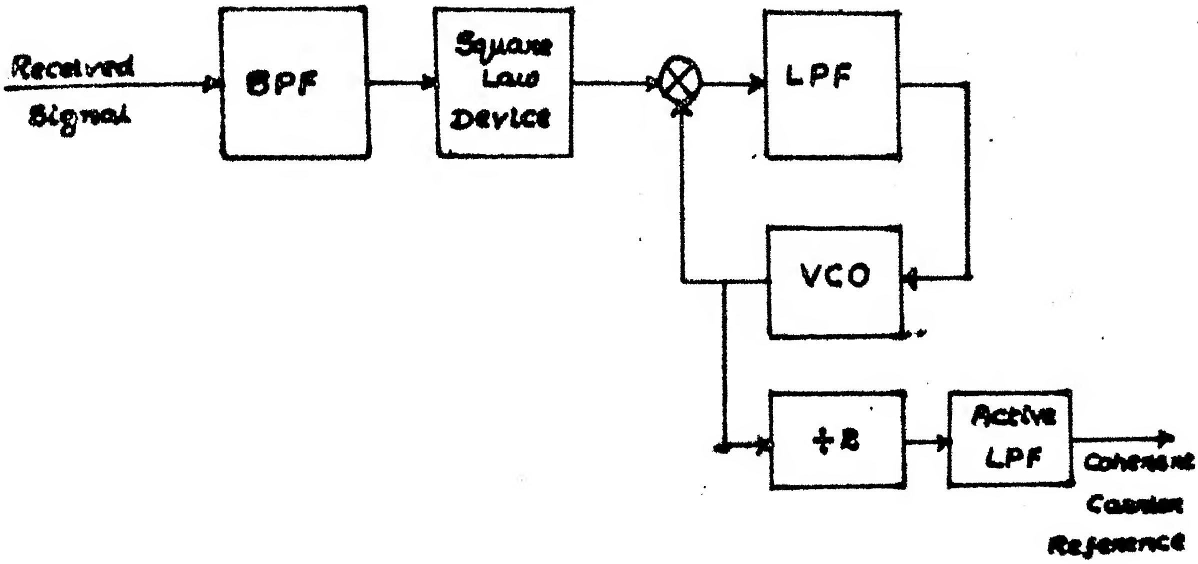

Fig 4·2 Block Diagram Of the Coherent Carrier Recovery Scheme

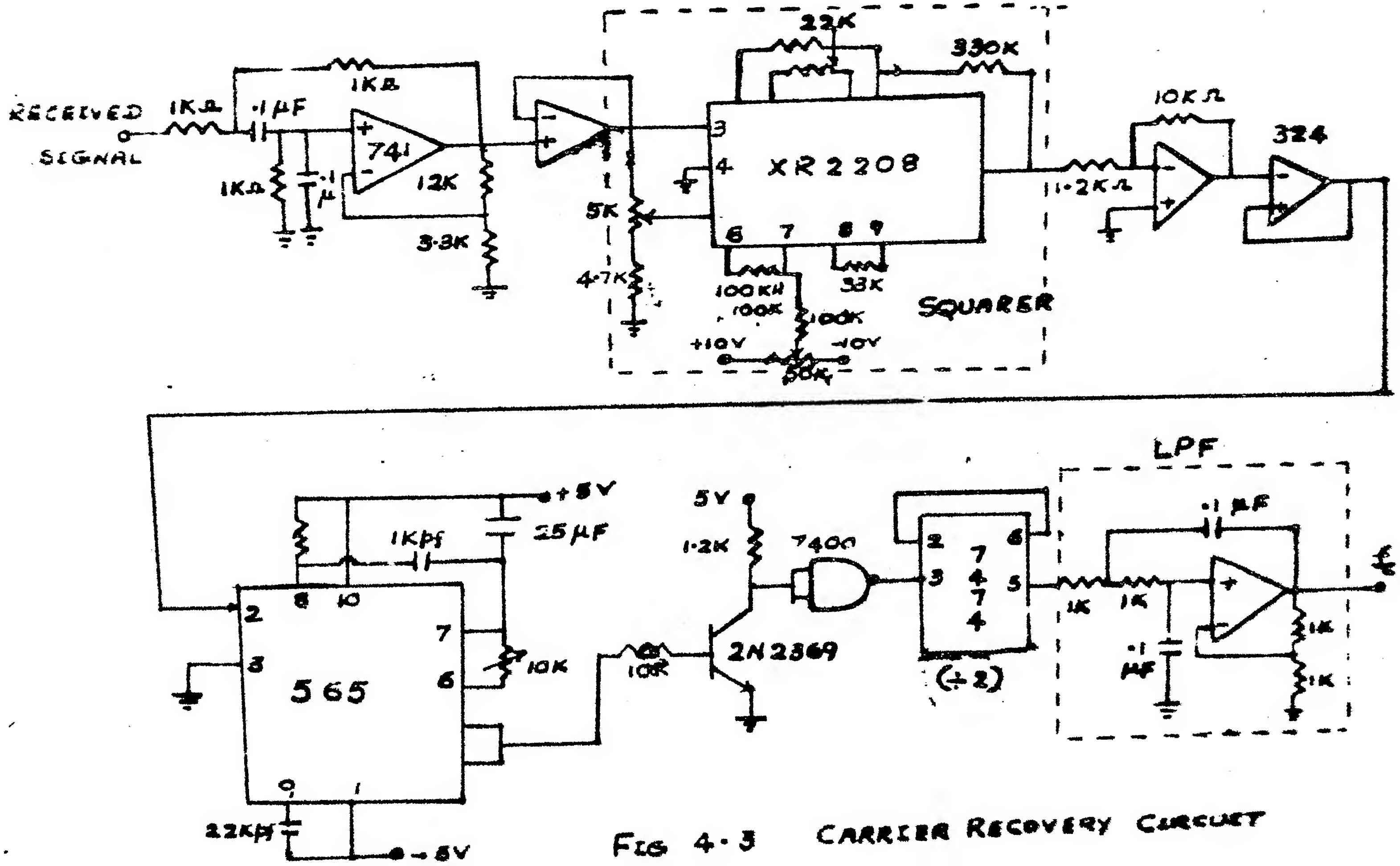

Fig 4·3 CARRIER RECOVERY CIRCUIT

amplifier and buffer and has a wide range of linearity. A simple bridge configuration can also be used to get the double frequency component. The offset adjustments of multiplier are not shown in Fig. 4.3.

4.2.1 Band Pass Filter Design

Centre frequency $f_o = 2.5$ kHz

Bandwith (B.W.) $= 360$ Hz

Therefore, $Q = \frac{f_o}{B.W.}$

$= 7$

Gain factor $K = 5 - \frac{\sqrt{2}}{Q} = 4.798$

$K = 1 + \frac{R_4}{R_5}$

The chosen values of R_4 and R_5 are

$R_4 = 12K \quad R_5 = 3.3\ K$

By setting $R_1 = R_2 = R_3 = R$

$C_1 = C_2 = C = .1\ \mu f$

$$R = \frac{\sqrt{2}}{\omega_o C} \left(\frac{\sqrt{2}}{2x\pi x2.5x10^3 x.1x10^{-6}}\right)$$

$= 1$ K Ohm

4.2.2 Phase Locked Loop Design

Centre frequency $f_o = 5$ kHz

Choosing $C_1 = 22$ Kpf

$R_1 = 2{\cdot}7$ K Ohms

By adjusting gain setting resistance between pins 6x7.

Lock range $= 2$ kHz

Therefore, capture range $= f_c = \frac{1}{2\pi}\sqrt{\frac{2\pi f_L}{\tau}} \approx 60$ Hz

where $\tau = 3.6 \times 10^3 \times C_2$.

4.3 PSK DEMODULATION

The recovered carrier is multiplied with the incoming modulated signal. The resulting signal is filtered and shaped to get an approximate SS code sequence.

A separate bit synchroniser is built for the recovery of the clock from the SS code sequence. Pulses are obtained at each transition of the sequence using two monostables and these are applied to PLL. As these pulses contain a spectral component of the original clock the PLL locks onto that component to give the clock.

Control signals required for integration and dumping are generated from this clock. The chips are decided by putting the threshold as zero on the decision device (comparator). The circuit diagram of PSK demodulation has been shown in Fig. 4.4.

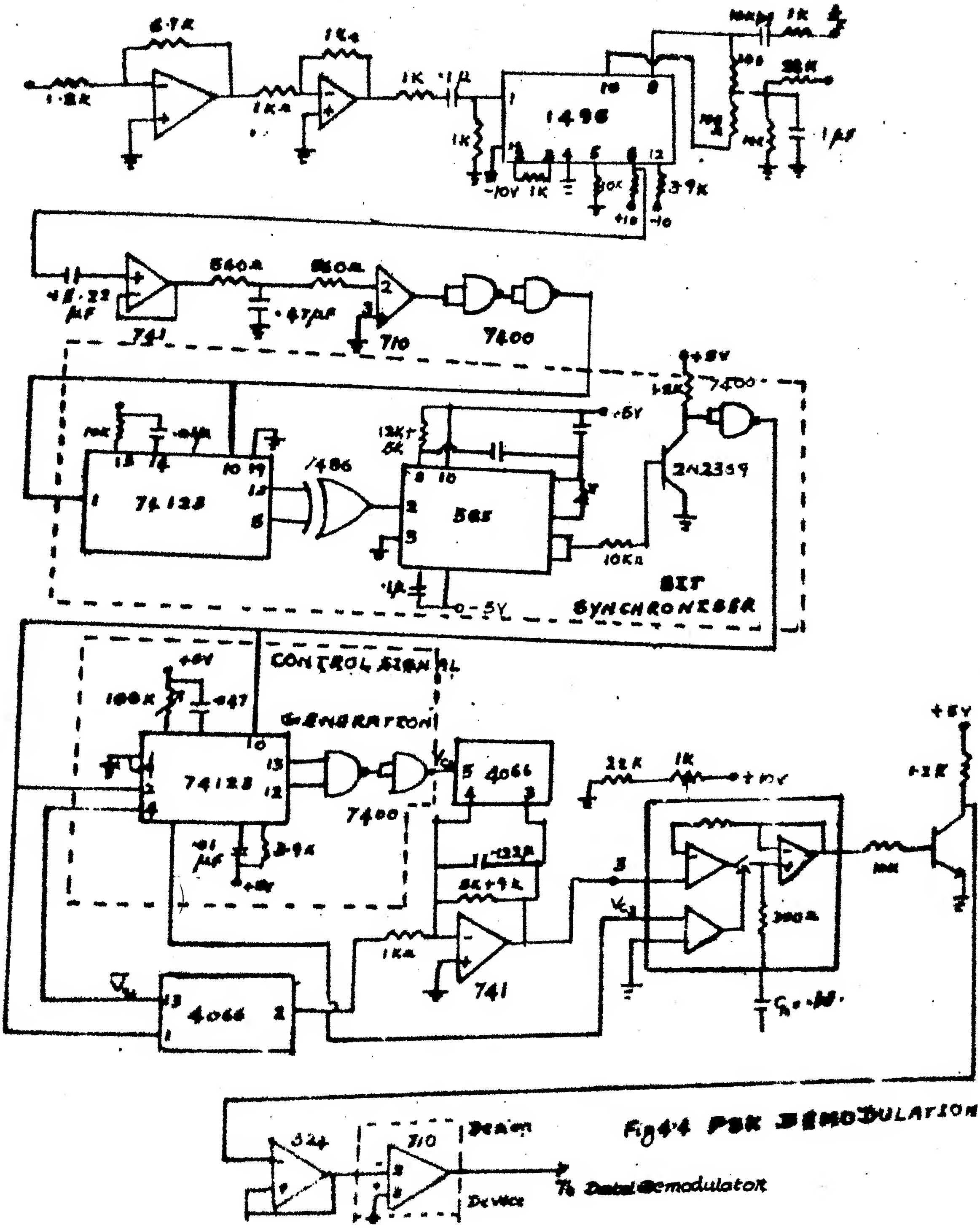

Fig 4.4 PSK DEMODULATION

4.3.1 Bit Synchroniser

The principle of deriving the clock has been shown in Fig. 4.5.

The centre frequency of the VCO = 180 Hz
(free running frequency) (f_o)

$$f_o = \frac{1.2}{4R_1C_1}$$

Choosing C_1 = .1 μF

$R_1 \approx$ 16.66 K Ohms

= 12K + 5 K

Choosing the gain setting resistance between pins 6,7 as 10 K.

Lock range f_L = 130 Hz

Therefore capture range f_c = 25 Hz

4.3.2 Integration and Dumping

The control signals required for integration and dumping are shown in Fig. 4.6. The threshold on the comparator is put as 'zero' for deciding the bits. The integrator shown in Fig. 4.4 is designed for a cut-off frequency of 180 Hz.

4.4 DATA DEMODULATION

The Data is demodulated using digital correlation technique. The block diagram of the data demodulator is shown in Fig. 4.7.

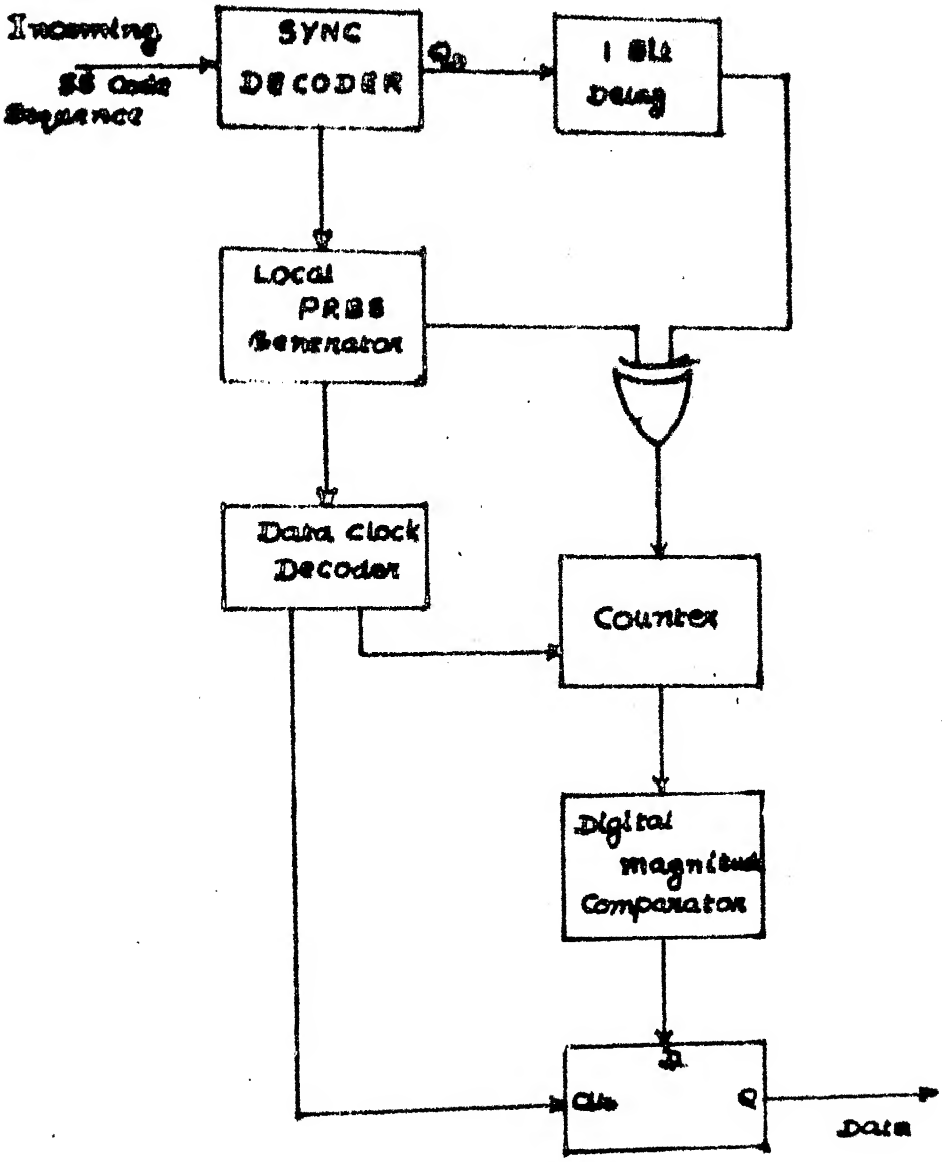

Fig 4·1 Block Diagram of the Data Demodulator

The incoming SS code sequence bits are shifted into a register. Whenever there are 4 ones or 4 zeros, the Sync. Decoder shown in Fig. 4.7 generates a pulse which sets the local PRBS. The preset data on local PRBS is 1111. The local PRBS is modulo-2 added to the incoming SS code sequence. The resulting bits are fed to a counter and digital magnitude comparator. The data bits are decided correctly even if there are 7 bit errors in a 15 bit frame of SS code sequence by putting a threshold on the comparator. The data clock is recovered and is used to enable the clock of the shift register and thus only the actual message bits are loaded in the latch.

The circuit diagram of the data demodulator is shown in Fig. 4.8.

The circuit has been tested by adding noise to the signal using Random Signal Noise Generator. With the transmitted signal amplitude 1 V_{p-p} by the addition of upto 0.5V noise the circuit has performed very well. When the signal amplitude has been increased to 1.5 V_{p-p}, even with addition of 1V noise the circuit performed well.

For asynchronous communication when there is no transmission, the inverter output will be essentially zero. When 1 followed by zero comes, then only the actual message bits are loaded in the latch. This feature though not implemented is shown in Fig. 4.9.

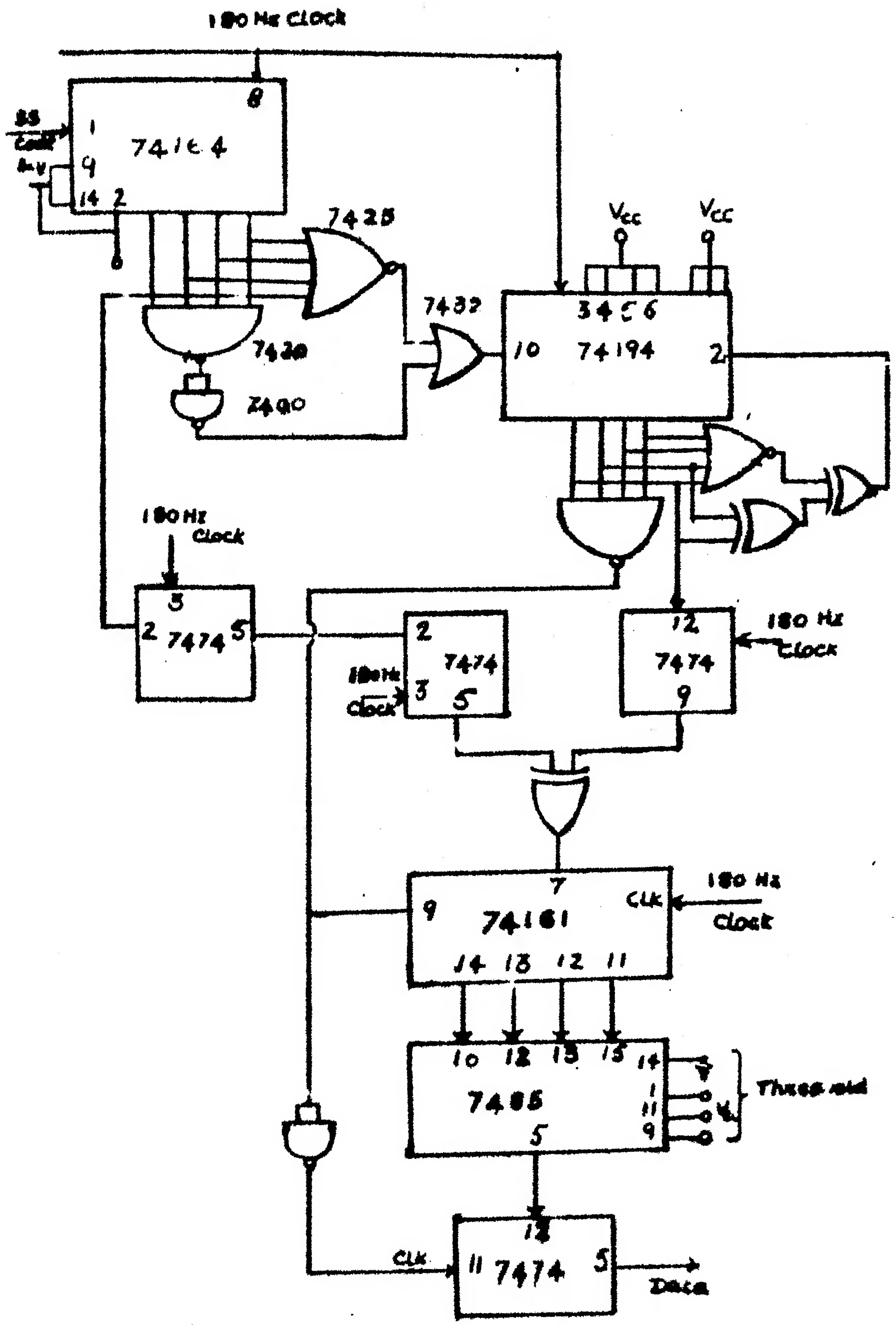

FIG 4.8 CIRCUIT DIAGRAM OF DATA DEMODULATOR

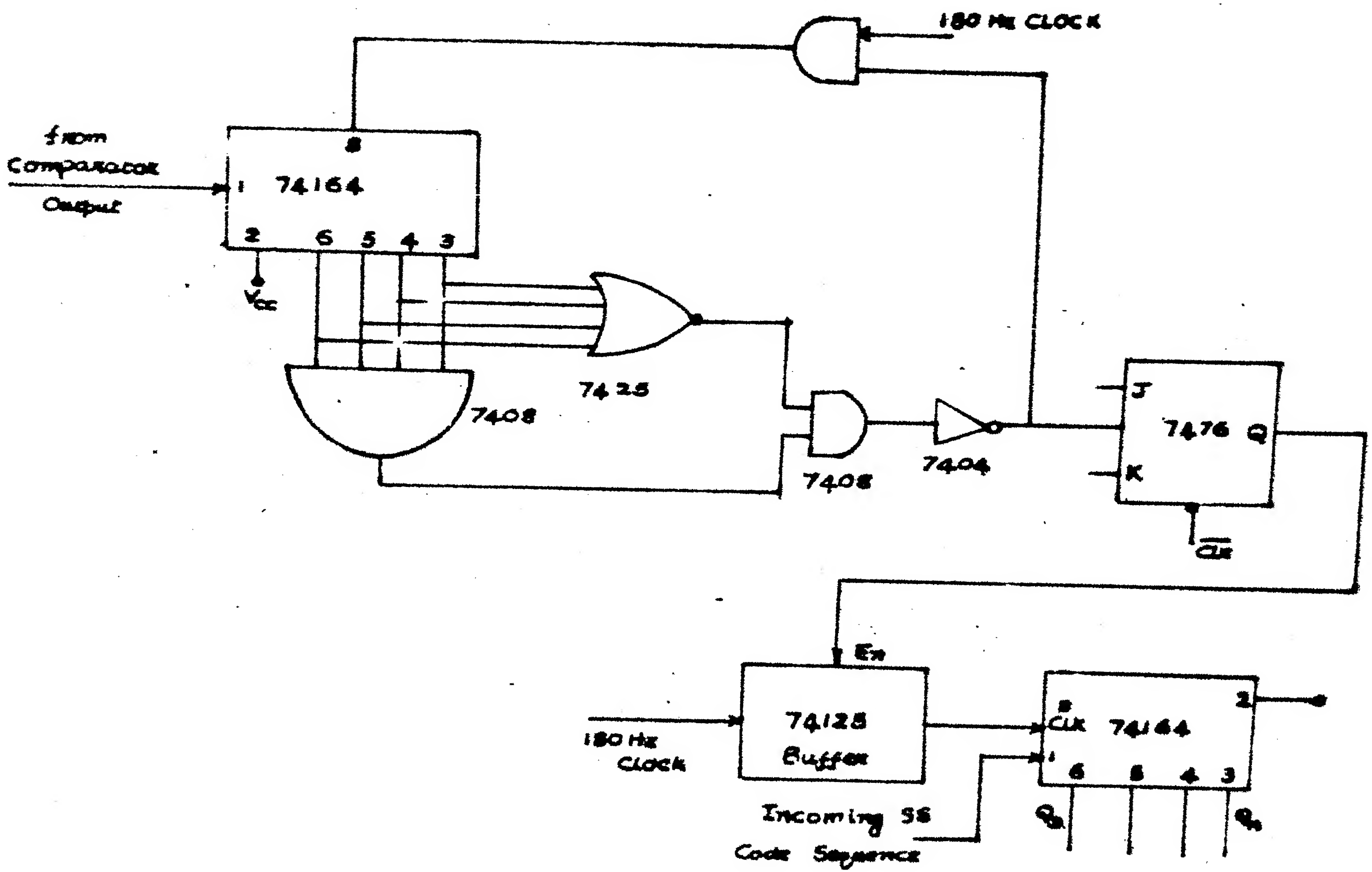

Fig 4-9 Circuit Diagram for the detection of 1 followed by 0 for asynchronous VLF Communication Receiver

CHAPTER 5

POST ANALYSIS OF SYSTEM DESIGNED

5.1 PRESENT LIMITATIONS

Complete performance tests have not been done. The system that has been constructed is only for a single user as 15 bit code length will provide only one channel. One can easily think of going for 31 bit code length which provides 3 channels. Instead of 16 Key encoder 74C922, a key encoder which can encode large number of keys, can be used. One elegant solution is using the single chip microcomputer 87C48 which is discussed later in this chapter. But this is also not available here.

5.2 SUGGESTIONS FOR FUTURE WORK

The recent developments in mines communications have been given by Durkin [13]. Various areas of investigation may lead to improved performance [14]. The first obvious choice is to increase the strength of the signal source. However, intrinsic safety considerations limit the output power (magnetic moment). Correlation techniques could be used employing an array of receiving antennas to improve detectability. Noise cancellation through correlation techniques involving the noise at the receiving antenna and a distant antenna outside the signals range is an area for future work.

Possibly the most promising venture to improve signal detectability is a project under investigation by Develco [15]. Here the underground transmitter transmits the signal continuously. The surface receiver uses a microcomputer which coherently integrates the transmitted signal. The principle idea is to exchange time for signal detectability. The receiver continuously monitors the signal and if it exists and is within the detectable range of the receiver it will eventually be detected.

5.2.1 Implementation of the System for Burst Mode Transmission

As far as the transmitter is concerned, the battery drainage is most important factor. For consumption of power it is better not to transmit anything when there is no transmission. But this causes serious problems as far as the receiver is concerned. As each PLL takes some time to lock on, by the time the PLL locks on the actual message bits are lost. So some scheme must be thought of for burst mode transmission.

Assuming some information has been sent initially for the PLL to lock on, then a scheme as shown in Fig. 5.1 can be used.

5.2.2 Delay Locked Loop Implementation

Once a spread spectrum receiver has synchronised with a received signal, it must continue to operate in such a way that it remains locked with its code reference exactly tracking the coded incoming signal. The two most common techniques for doing this are tau-dither and delay lock.

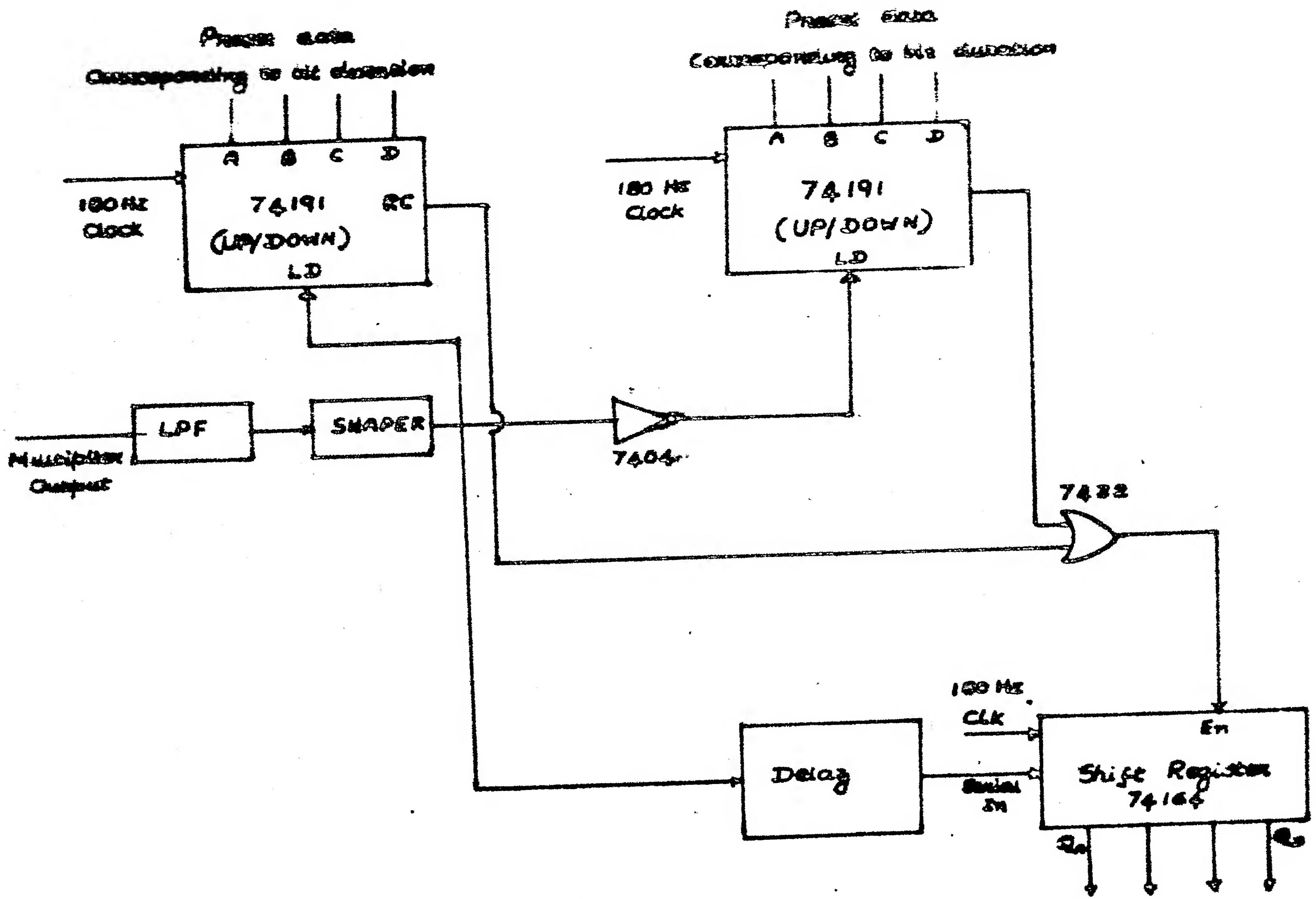

Fig 6.1 Receiver Modification Circuit diagram for Burst Mode Transmission

The delay locked loop has been constructed and tested. The circuit diagram has been shown in Fig. 5.2.

In delay lock loop two local reference signals are generated. The amount of delay between the local codes is usually 1 or 2 bits. The references are used for comparison with a single incoming signal in two separate correlators. The correlator outputs are summed and filtered and used to control the receiver's clock source (VCO), the receivers code will track the incoming code at a point half way between the maximum and minimum of composite correlator output.

5.2.3 Simulation on Workstation

The entire DSSS system can be simulated using a computer [16].

The receiver is simulated on work station. A flow chart of the simulation work is shown in Fig. 5.3.

5.2.4 Using 87C48 and 2920 in the Transmitter and Receiver Respectively

Using the CMOS single chip microcomputer 87C48 the key-board scan, the detection, the encoding and the generation and transmission of frequencies will all be done under software control. For the SS system there is flexibility of changing code length.

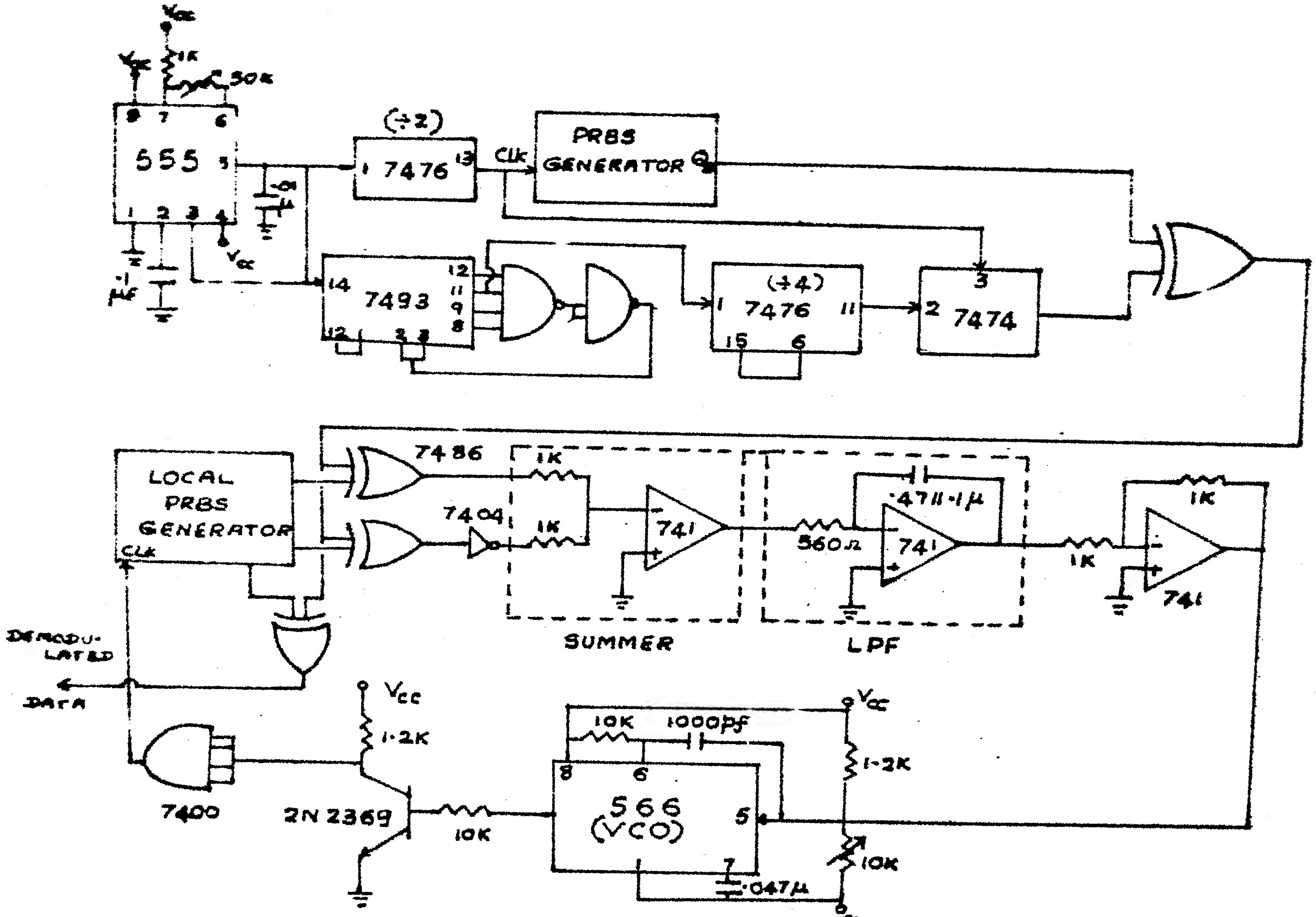

FIG 5·2 DELAY LOCKED LOOP

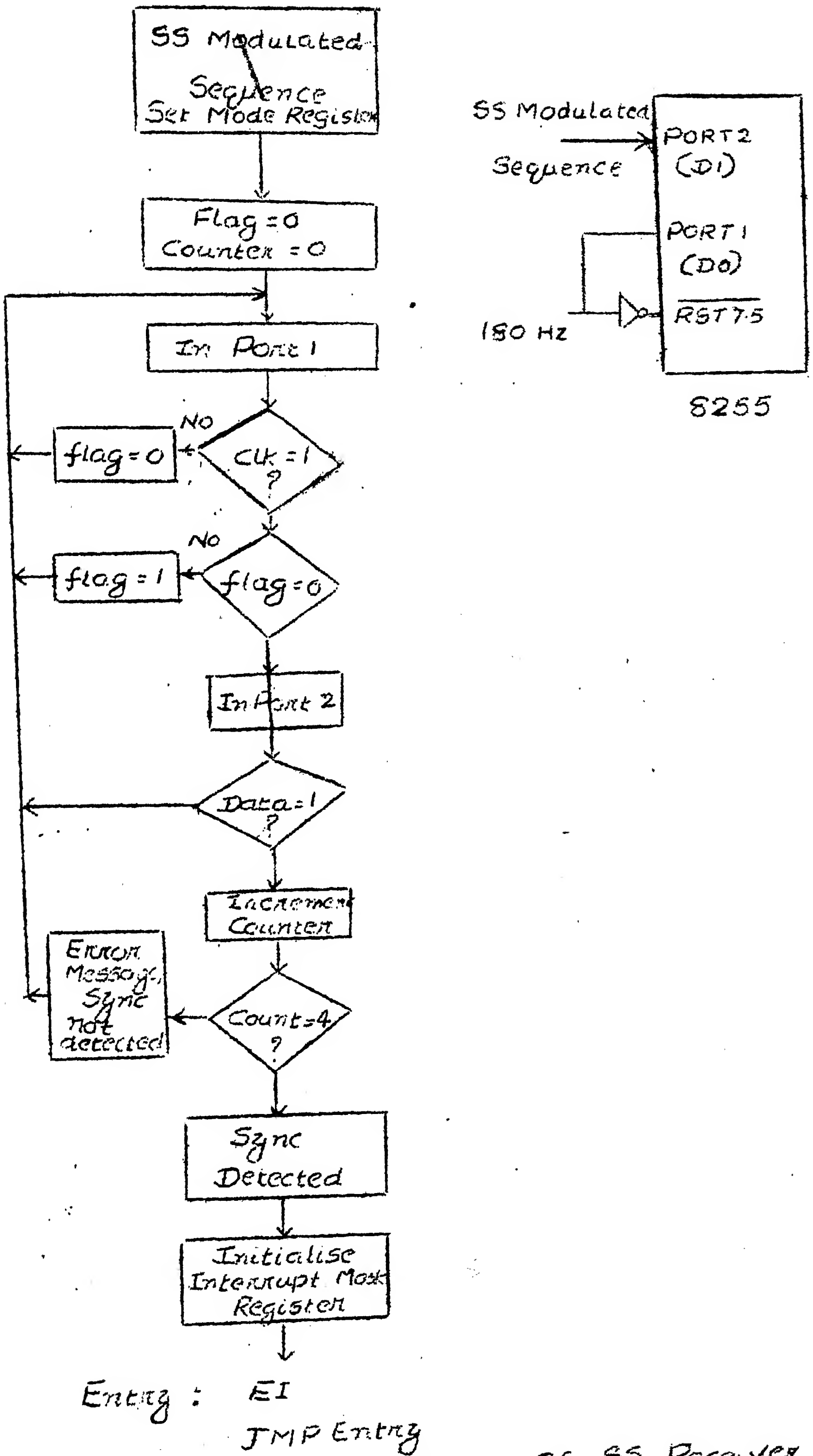

Fig 5.3 Flow Chart for Simulation of SS Receiver

ISS:

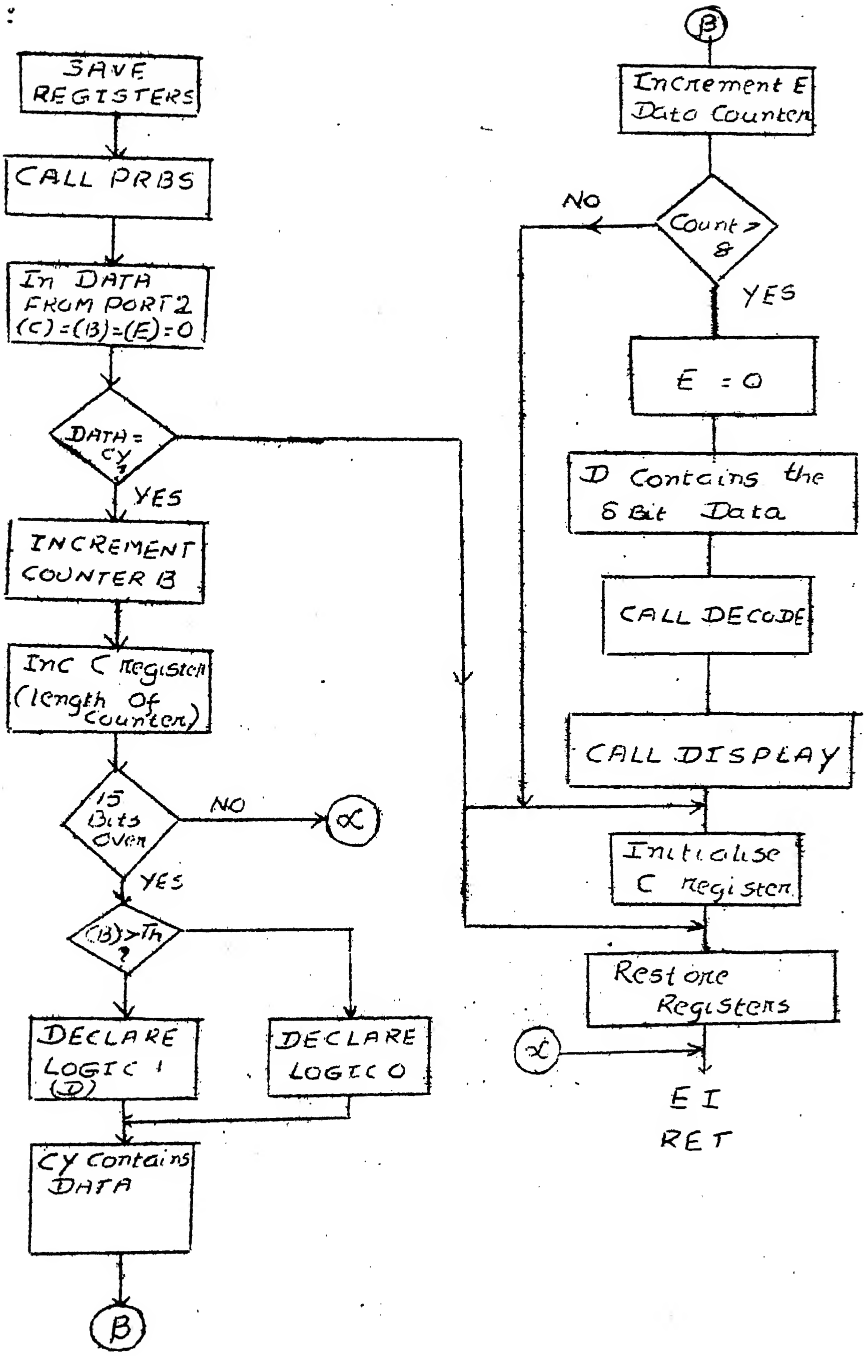
SAVE REGISTERS
CALL PRBS
In DATA FROM PORT 2 (C)=(B)=(E)=0
DATA = CY ?
YES
INCREMENT COUNTER B
Inc C register (length of counter)
15 Bits over
NO
YES
(B)>Th ?
DECLARE LOGIC 1 (D)
DECLARE LOGIC 0
CY contains DATA
B
Increment E Data Counter
Count > 8
NO
YES
E := 0
D contains the 8 Bit Data
CALL DECODE
CALL DISPLAY
Initialise C register
Restore Registers
EI
RET

The noncoherent FSK transmitter using 8748 has already been done [17]. The entire SS receiver can be implemented using the analog signal processor 2920.

Frequency shift keying is typically used for low to medium speed applications. The 2920 Application note discusses the implementation of low to medium speed frequency shift keyed modems using 2920 Analog signal processor [18]. The full software has been given in it for typical data rates.

5.2.5 Using Speech Synthesizer

Speech synthesizer SC-01 can be used to get the audio output corresponding to the key depressed.

The serial data from the data demodulator is first latched onto a port. A microprocessor is used inconjunction with the speech synthesizer. The processor first reads the codes from the input port. It first stores them in a RAM then it will take each code one by one and decode them to get the memory locations where the starting address of the phonem sequence of the word is stored. Then it reads the phonems for the word from the EPROM and outputs them sequentially to SC-01 performing proper handshake to produce the audio output corresponding to that word.

Alternatively LEDs can be used to indicate the depressed key.

5.3 CONCLUSIONS

The feasibility of using SS Modulation for through the earth communication has been studied. SS can be used to reduce the dominant source of noise, power line harmonic interference.SS is reliable in the sense that even if a few harmonics fall in the band, due to the power line frequency instability, the signal can be detected because of its processing gain capability. This feature is lacking in other digital data systems.

REFERENCES

[1] J. Durkin, 'Electromagnetic Detection of Trapped Miners', IEEE Communications Magazine, vol.22, pp 37-46, February 1984.

[2] Simon Ramo, John R. Whinnery, Theodore Van Duzer, Wiley Eastern Private Limited, 1965.

[3] Trapped Miner Location Communication System Development Program, NTIS, May 1970.

[4] The Third WVU Conference on Coal Mine Electro Technology, August, 1976.

[5] The Fifth WVU Conference on Coal Mine Electro Technology, August 1978.

[6] Trapped Miner Location Communication System Development Program, vol. III, Westinghouse Electric Corporation, NTIS, May 1973.

[7] R.C. Dixon, 'Spread Spectrum Systems', A Wiley Inter-science Publication, 1976.

[8] J.N. Murphy and H.E. Parkinson, 'Underground Mine Communications', Proc. IEEE, vol. 66, 1978.

[9] J.R. Wait and L.L. Campbell, 'The Fields of an Oscillating Magnetic Dipole Immersed in a Semi-Infinite Conducting Medium', JGR, vol. 58, pp 167-178, June 1953.

[10] A.K. Sinha and P.K. Bhattacharya, 'Vertical Magnetic Dipole Buried Inside a Homogeneous Earth', Radio Science, vol. 1, No.3, March 1966.

[11] Simon Haykin, Communication Systems, Wiley Eastern Limited, 1978.

[12] Jim K. Omura and Paul D. Shaft, 'Modem Performance in VLF Atmospheric Noise', IEEE Trans. on Commns. vol.COM-19, Oct. 1971.

[13] J. Durkin, Electromagnetic Detection of Trapped Miners, IEEE Communications Magazine, February 1984.

[14] 'A Study for the Detection of Weak Electromagnetic Signal Bursts with Hard-Limited Arrays', Final Rept., Bureau of Mines Contract, Dec. 1980.

[15] Develco, 'EM Rescue System for Deep Mines', Final Rept., Bureau of Mines, May 1979.

[16] J.R. Sergo and J.F. Hayes, 'Analysis and Simulation of pn Synchronisation System', IEEE Trans. Comm. Tech. Oct. 1970.

[17] Harishankar and Sanjiv Nanda, 'VLF Transmitter Based on Single Chip Microcomputer', 1983.

[18] Intel's Application Note on 2920 Signal Processor in Modem Applications, June 1981.

EE-1984 - ~~M~~ KUM - WYR